ACOUSTIC EMISSION DETECTION AND SOURCE LOCATION

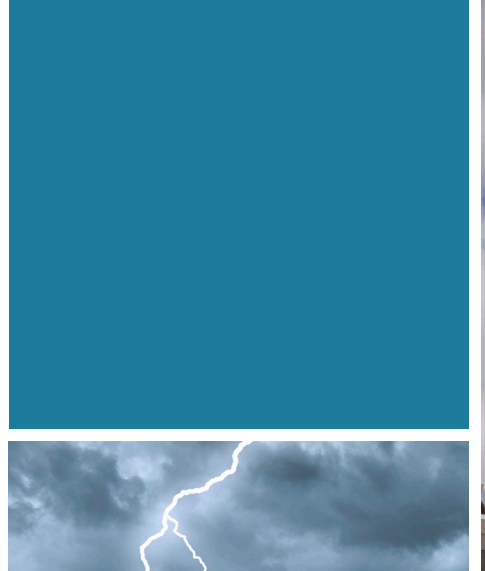
REPORT 2020:697







BETONGTEKNISKT PROGRAM KÄRNKRAFT









Acoustic Emission Detection and Source Location

Findings in the Ringhals 2 reactor containment during pressure test

PETER ULRIKSEN KARIM HADDAD JOHANNA SPÅLS

Förord

With an ageing fleet of nuclear reactors, finding non-destructive methods to ensure the integrity of the reactor containment with cast-in liner is important. Detection using acoustic emission to locate anomalies in the construction, could be a possible global method to identify areas that can be further investigated using local investigation methods.

The method of acoustic emission detection to locate areas that emit sound events during pressure test has been tested in the reactor containment of Ringhals 2. A team with Professor Peter Ulriksen at Lund University and senior experts Harim Haddad at Brüel and Kjaer Sound and Vibration and Johanna Spåls at Ringhals carried out the project. Sound events could be a sign of an anomaly in the construction, for example corrosion in the liner.

This project was been carried out in the Energiforsk Nuclear Concrete Research Program, with stakeholders Vattenfall, Uniper/Sydkraft Nuclear, Fortum, Teollisuuden Voima Oy (TVO), Skellefteå Kraft, Karlstads Energi and the Swedish Radiation Safety Authority (SSM).



Sammanfattning

Inom NUGENIA-ACCEPPT projektet studerades metoder för att globalt och lokalt identifiera skador i invändigt placerad tätplåt i reaktorinneslutningar, såväl etablerade metoder som eventuellt nya. En av de nya globala metoderna som föreslogs var att lyssna på luftburna akustiska emissioner med mikrofoner, i stället för med fast monteradeaccelerometrar som mäter stomljud (AE).

Den föreslagna metoden testades 2014 under täthetsprov 4 atö i en fransk reaktorinneslutning. Detta försök bekräftade att det verkligen förekommer akustiska ljudemissioner som kan detekteras med mikrofon.

Med stöd i detta uppmuntrande resultat byggdes en tetrahederformad mikrofonarray, med vars hjälp det är möjligt att även bestämma riktningen till de registrerade akustiska emissionerna härkomst. Det sker genom att man bestämmer tidsskillnaden mellan emissionernas ankomst till de olika mikrofonerna.

Detta system testades 2015 i det ljudhårda rummet vid V-sektionen på LTH genom att en liten knäppare fördes runt på de kakelklädda väggarna i ett bestämt mönster. Testet skedde i samarbete med Brüel&Kjaer, som utvecklat liknande utrustning och mjukvara för utvärdering. Det visade sig att noggrannheten var utomordentlig.

Under vintern 2020 beslöts att genomföra ett täthetsprov i den avstängda reaktorn Ringhals 2 reaktorinneslutning. I månadsskiftet mars-april 2020 installerades den akustiska utrustningen av Ringhals grupp för mätteknik. 80 timmar akustiska data spelades in mellan det att personslussen till reaktorinneslutningen stängs och den åter öppnas efter täthetsprovet. Då den akustiska bakgrundsnivån är för hög under tryckupptagning och trycknedtagning är det endast mellan dessa faser (stabilisering samt mätperiod) som inspelningen är användbar.

Under den analyserade perioden kunde 59 akustiska händelser riktningsbestämmas med god säkerhet av de c:a 200 transienter som kunde detekteras med en automatisk algoritm.



Summary

Within the NUGENIA-ACCEPT project Peter Ulriksen at LTH was given the task of investigating established methods for global and local investigation of damages in the inside surface-mounted liner plate and to suggest new methods. One of the suggested global methods was to listen for airborne acoustic emissions with microphones, instead with fixed installations of accelerometers measuring structural emissions. Karim Haddad at Brüel&Kjaer has developed hardware and software to locate airborne emissions and a cooperation has taken place in this project. Johanna Spåls at Ringhals orchestrated the acoustical tests there.

The suggested method was tested in a French reactor containment during a pressure test in 2015. This test confirmed that there really are acoustic emissions that can be detected with a microphone.

Supported by this encouraging result a tetrahedral microphone array with four microphones was constructed, which makes it possible to determine the directions from which the transient emissions are emanating. This is done by determining the difference in arrival time of the emissions to the different microphones.

The new system was tested in the reverberation chamber in Civil Engineering at LTH. A small device emitting transients was moved around the walls of the echoic chamber in a specified pattern. This test was performed in cooperation with Karim Haddad Brüel&Kjaer Denmark that had developed similar equipment and software for evaluation. It turned out that the precision in localization was extremely good.

In Mars-April of 2020 a pressure test was planned in the decommissioned Ringhals 2 reactor containment in Sweden. This was an opportunity to piggy-back a long planned acoustic test with four microphones. The acoustic test implementation was orchestrated by Johanna Spåls at the Nuclear Power Plant. After instructions the developed equipment was installed by the Ringhals measurement group. 80 hours of acoustical data was recorded between the closure of the personal sluice before the pressure test and the subsequent opening, when the air pressure had dropped to normal again. Only the period between the end of the compression phase and the beginning of the decompression phase is useful for the analysis of emissions, during the compression/decompression phases the acoustic background level is too high.

An automatic transient detection algorithm found 200 acoustic emissions. Out of these 84 were manually / visibly selected for further analysis. Out of these, 59 emissions could be localized with high confidence, using a correlation method to find differences in arrival times. Most of these emanates from the dome where the liner is surface mounted.



List of content

1	General Introduction		7
2	Performing the pressure test and the acoustic recording		
3	Reco	12	
4	Anal	16	
	4.1	Extracting events	16
	4.2	Calculating the direction to the source of events	22
5	Intro	duction to direction finding	25
6	Micr	ophone array and convention	26
7	Proc	essing of the microphone signals	29
	7.1	The signals	29
	7.2	Array Processing	30
	7.3	Assumptions	30
8	Results		32
	8.1	Overall Results	32
	8.2	Individual results	33
9	Conc	lusions	34
10	References		35
Appe	Appendix A: Attachment 1 Technical manual (in Swedish)		
Appe	Appendix B: Attachment 2 Individual Event Location		



1 General Introduction

In the NUGENIA-ACCEPPT WP1-G2 (1) project Peter Ulriksen, one of the authors of this report, was given the task of writing an overview of established methods possible to use in global and local surveys of the inside surface mounted liner in nuclear power plant (NPP) reactor containments. Airborne acoustic emission detection was one new method suggested for global detection.

The underlying idea was that deformations in the liner's welds and shear deformation between liner and concrete should generate acoustic emissions that could be detected with microphones. If four microphones in a tetrahedral array configuration was used the direction to the source of the emission could be calculated using back-projection.

In order to see if this was feasible a test was made in a French NPP during a pressure test in December 2014. The recording was made with a digital recorder ZOOM H6 and a condenser microphone of type JM27. The test confirmed that gunshot like acoustic emissions were present.

Subsequently an acoustic array with four microphones were constructed, see Figure 1.

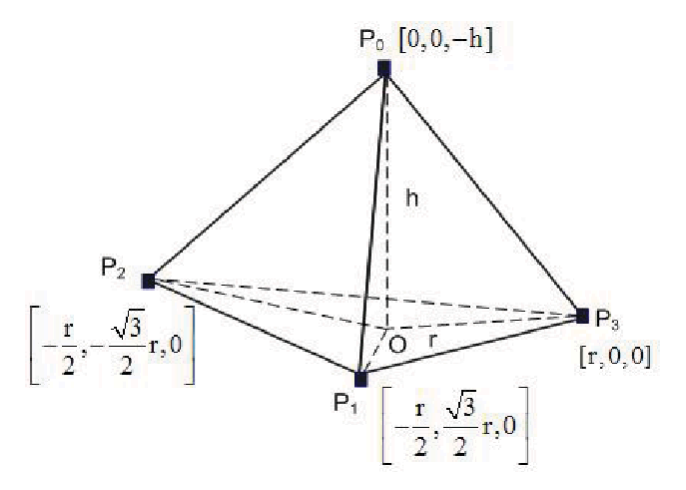


Figure 1: Standard view of a tetraheder. In this orientation it looks more complicated than it is. It is a matter of two orthogonal microphone booms P0-P1 and P2-P3 with a separation in elevation

With this microphone orientation the direction in 3D to the source of a transient emission can be calculated using the difference in arrival times to the four microphones.

This setup was then tested in the reverberation chamber at LTH in 2015. This chamber, all surfaces covered in tiles, supposedly has the same properties as an NPP reactor containment. The tests were performed together with Jørgen Hald and Karim Haddad at Brüel&Kjaer in Denmark. They had developed both hardware and software for similar measurements.



An impulsive sound source was moved in a specific pattern along the wall and the signals recorded with the same kind of recording equipment as used in the French NPP experiment. The analysis showed that the location of the transients could be determined with high accuracy, see Figures 2 and 3.



Figure 2: Arrangement of the tetrahedral array in the reverberant chamber.

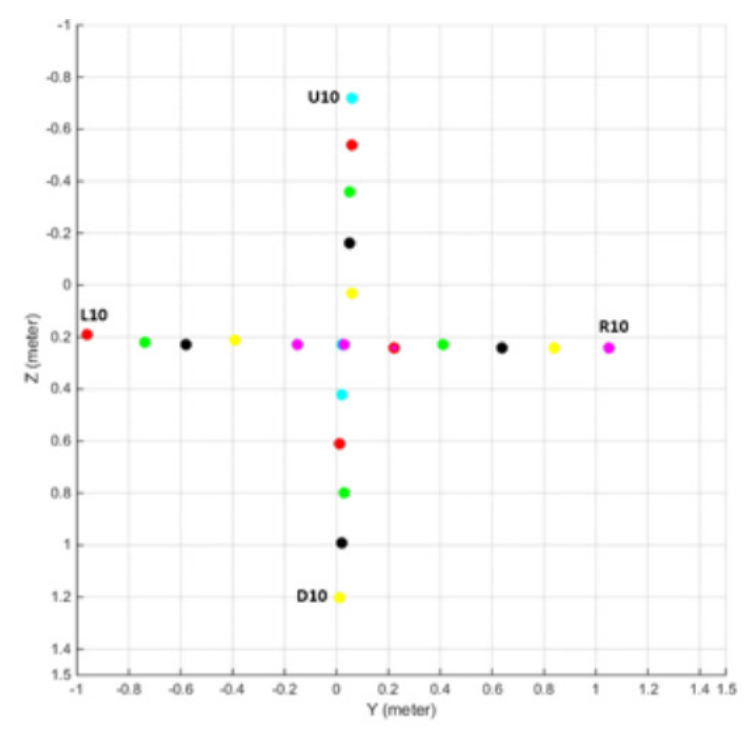


Figure 3: Calculated positions of the impulsive source. Truth is a straight cross with identical distances between points.



During the winter 2020 it was determined that a pressure test should be performed in the decommissioned NPP Ringhals 2 reactor containment. An additional acoustic recording was the orchestrated by Johanna Spåls at Ringhals. In anticipation of this opportunity a digital recorder with increased capacity was replacing the previously used ZOOM H6. The new recorder is a ZOOM F8, with 2 x 512 GB capacity. This was necessary since a several days long recording with four microphones at two sensitivity levels takes up a lot of memory space. A sealed steel box for the recorder was also constructed, mostly as a protection in case of fire in the recorder. The new version of the instrument was delivered to Ringhals March 26 2020 and a short introduction was given to the Measurement group, Figure 4. Also a written introduction was handed over, it can be read in Attachment 1.

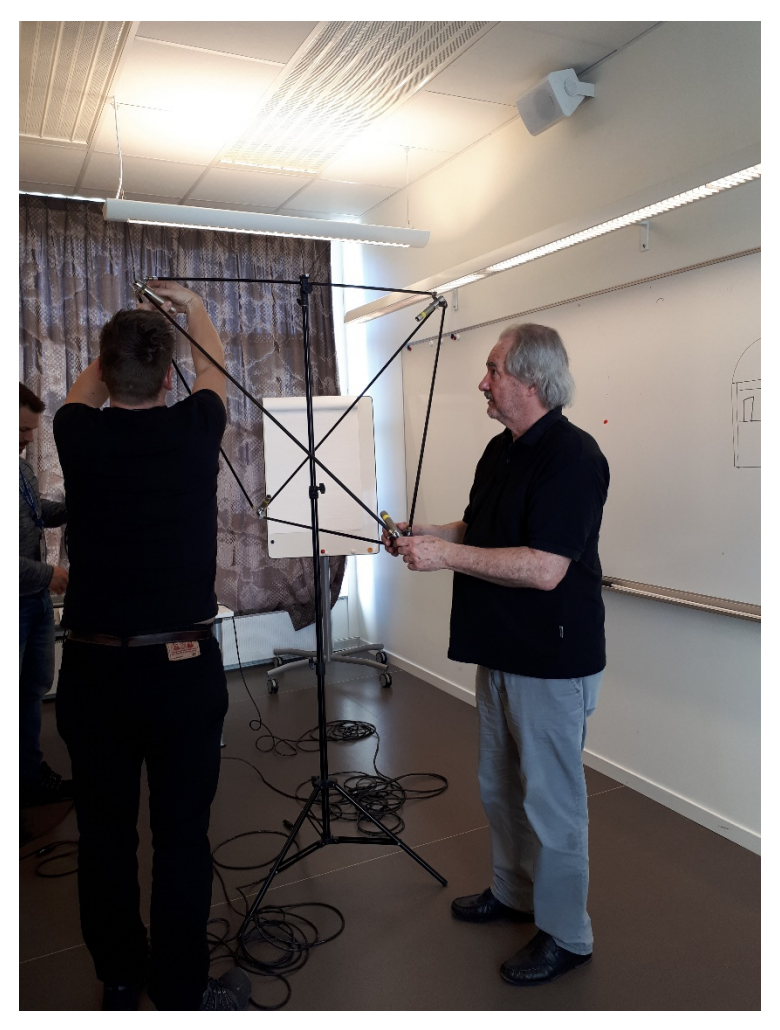


Figure 4: Instruction in how to assemble the array of four microphones.



2 Performing the pressure test and the acoustic recording

The installation of the recording equipment was made by the Ringhals measurement group. It was previously agreed that the microphone array should be placed on top of one of the cantilevers for the polar traverse.

In this way there would be an unobstructed view from the microphone array to every point in the dome, where the liner is inside surface mounted, see Figure 5 and 6. This is not the case in other parts of the containment, where the liner is concealed by concrete.



Figure 5: The microphone array - located where the black arrow indicates.

The recording must start before the person sluice to the containment is closed. This means there will be a long period of recording meaningless sounds. Considerable time later the compression phase starts. This generates very strong noise rendering it impossible to record anything else. When the test pressure is reached the compression stops and the stabilizing and measurement period starts. After the compression stops it is rather quiet in the containment and meaningful acoustic signals can be recorded and analyzed. This productive period ends when the air pressure is released and a similar noisy period starts until the person sluice can be opened again at normal pressure and the recording stopped.



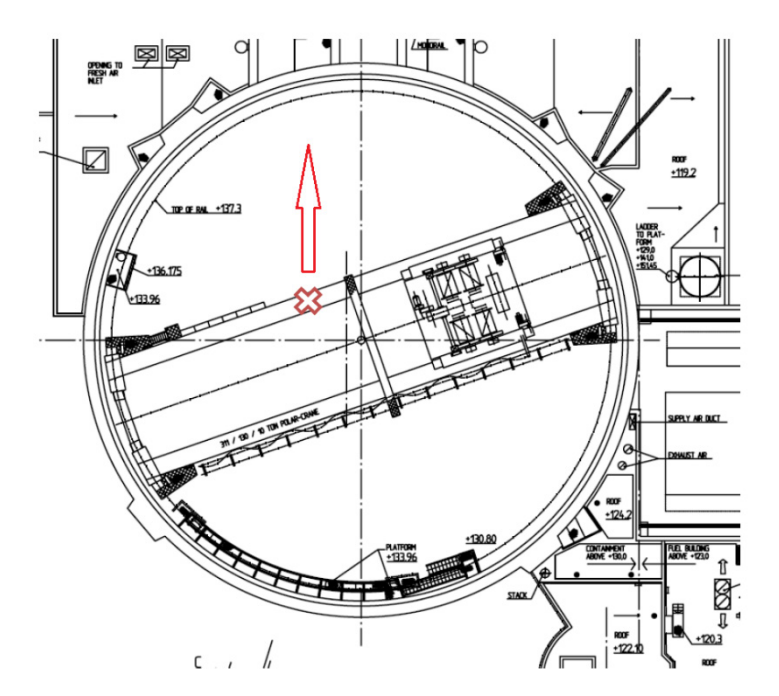
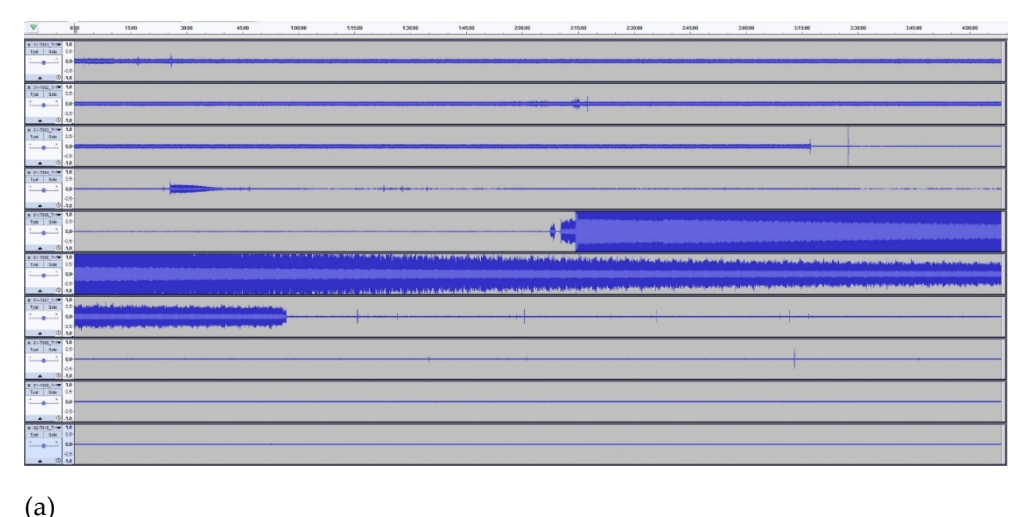


Figure 6: The location of the microphone array in the plane of the traverse cantilever plane. The arrow indicates the direction of the upper microphone boom microphone 1.



3 Recorded signals

The digital recording was made at two different sensitivity levels for each microphone. This is a convenient possibility with the ZOOM F8 recorder. This was made since the actual sound level in the containment under pressure was not known beforehand. <this means that there is a double set-up of recordings. Apart from that the recorded data was also transferred to two different 512 GB SD-cards in real time, for security reasons. The data quality in all recordings was 24 bits at 48 kSa/s. The recorder breaks up the data in 4hour 8 minutes and 30 seconds epochs. There were 20 epochs recorded, i.e. about 80 hours of recording. Acoustic events have been identified using the AUDACITY freeware. Output from this software, covering the entire recording in channel 1, is presented in Figure 7a and b.



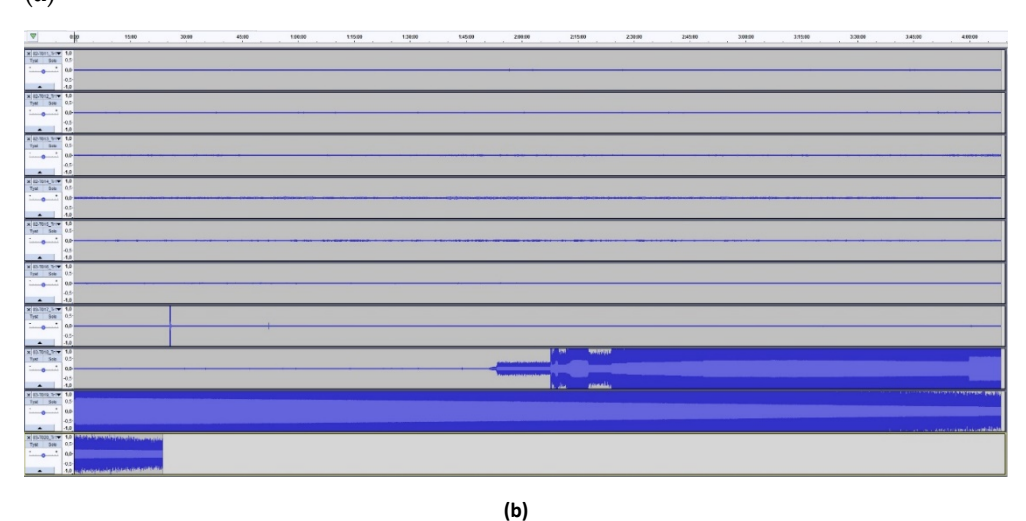


Figure 7. (a): The first ten epochs recording in channel 1 of the four channels. The strong amplitudes correspond to the compression phase. The lighter blue part of the signal is the RMS-value. The useful period starts after 25% of the 7th epoch, fourth from below. (b): The last ten epochs signal from microphone 1. The strong amplitudes correspond to the decompression phase.

To illustrate the acoustic emissions the amplitude has been increased in the diagram below, see Figure 8.



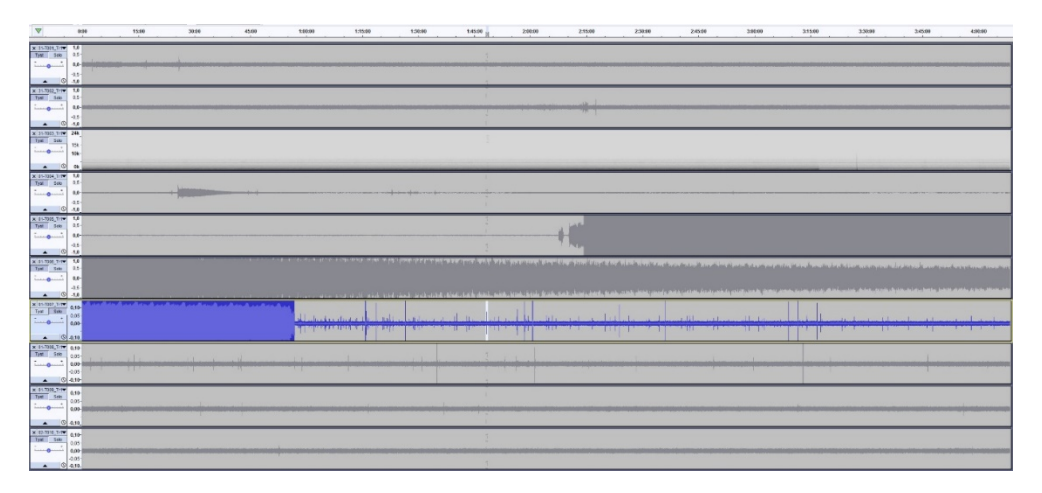


Figure 8: In this diagram the amplitude in epoch 7 has been increased tenfold to enhance the impulsive acoustic emission events.

A comparison between recordings with high and low sensitivity are given below, see Figure 9. During the period when the recording is saturated in the high sensitivity diagrams, the upper two, no analysis can be made. In order to check if there are any emissions in these epochs the low sensitivity recording must be used, the lower two. However no transients were identified in these epochs.

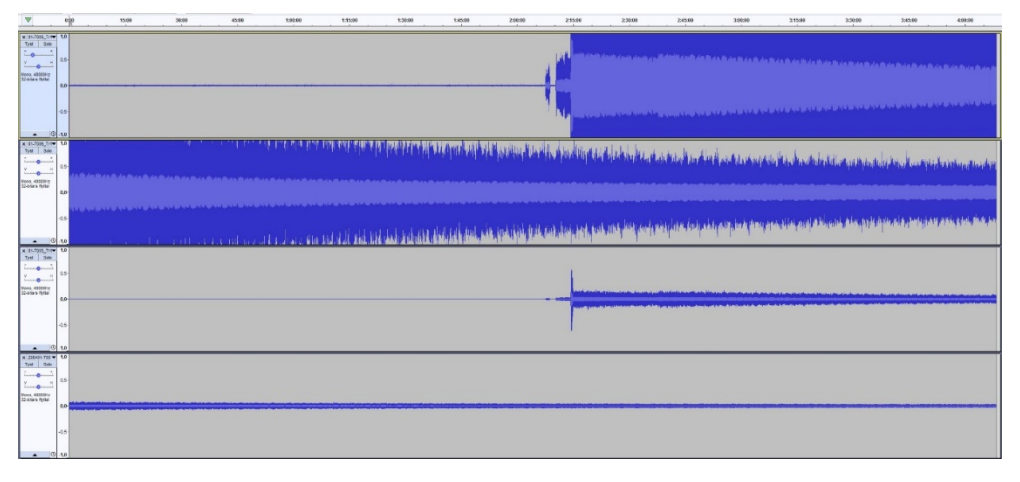


Figure 9: Comparison between a high sensitivity (upper two) and a low sensitivity (lower two) diagrams. The presented signals come from microphone 1 during epochs 5 and 6.

Each acoustic event consists of signals from the four channels the four microphones are connected to, see Figure 10. The property that has to be determined is the difference in arrival times of the transient sound to the four microphones. Knowing this makes it possible to calculate the origin of each emission using a mathematical process called beamforming. The difference can be manually picked from the first flank, the first zero-crossing or through cross correlating the extracted events. If first arrivals are used reflections can create no problems because they always arrive later than the direct path signals. Nothing from below the floor under the array can be calculated, see Figure 11. A



considerable part of the signals is reverberation, which makes it a prudent task to select the length of signal that should be correlated.

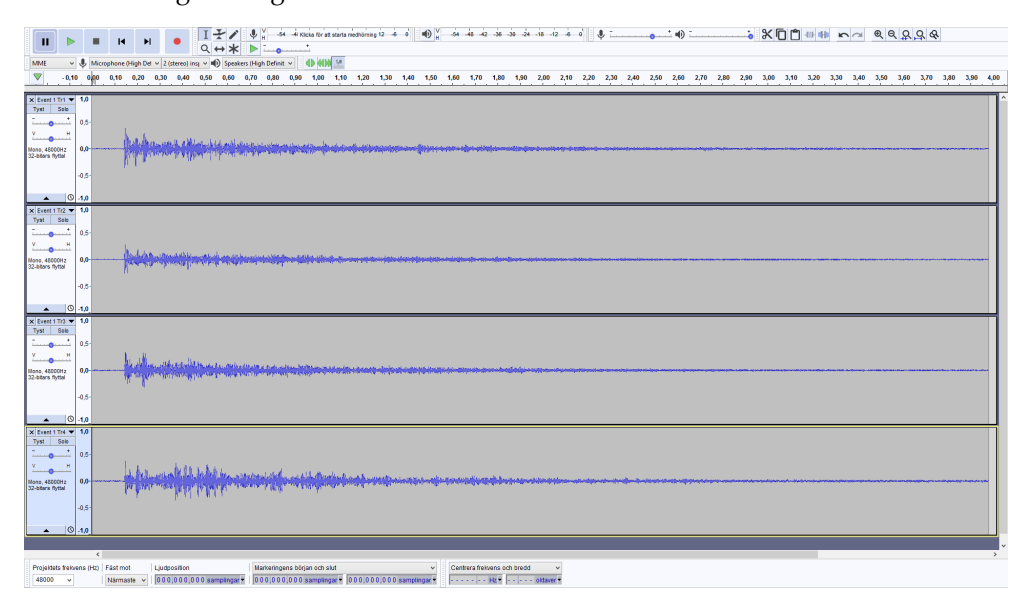


Figure 10: A complete four channel set of data for the extracted event number 1. These are typically 3-4 seconds long. With 48 kSa/s/ch this means that there are almost 200.000 samples in each channel.

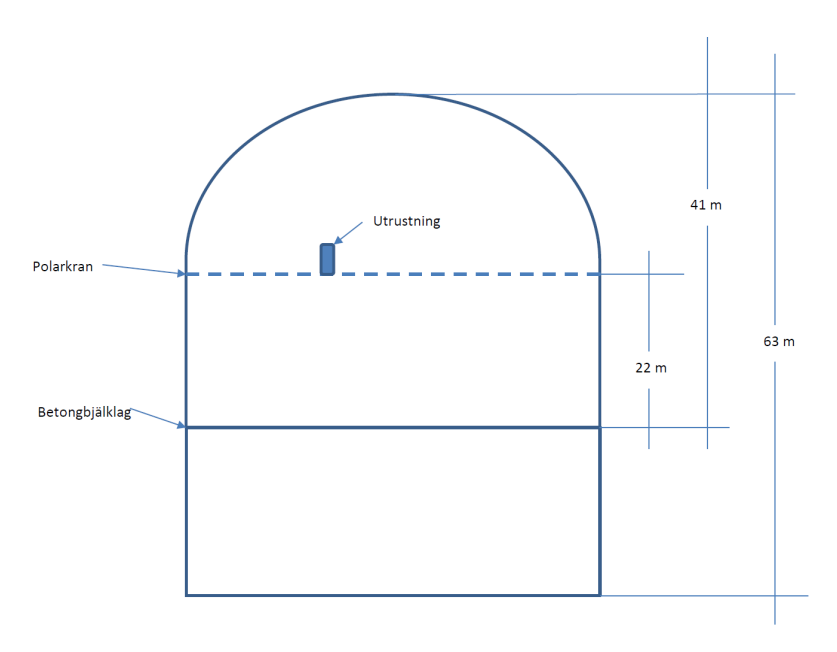


Figure 11: . Cross section through the reactor containment. The blue rectangle identifies the location of the microphone array. Above this the space is 19m, below it is 22 m to the floor. Under the floor surface there is another 22 m from which no emissions can be used for locating. The method can be said to be of the line of sight type, like a camera.

Below is a highly magnified version of the beginning of the signals in Figure 10. At that degree of magnification it is obvious that the signals arrive at different times, see Figure 12.



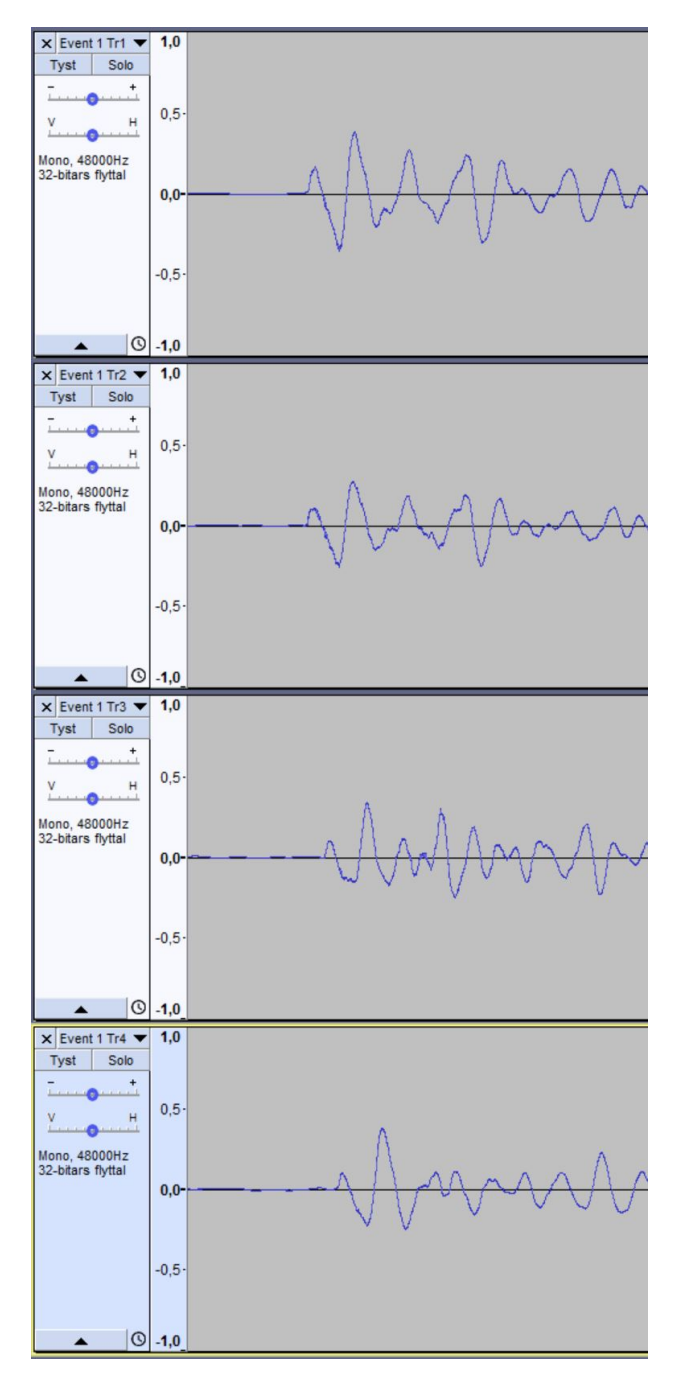


Figure 12: Magnified version of signals in Figure 10. The difference in arrival times is visible at this scale.



4 Analysis of the recorded signals

The analysis is performed in two steps. First all events are identified, extracted and classified on the basis of amplitude in a subjective manner. Then the source direction to each event is calculated.

The first part is done by Peter Ulriksen at LTH, the second part is done by Karim Haddad at Brüel&Kjaer.

4.1 EXTRACTING EVENTS

In the 20 epochs recorded the first 6 and the last 3 contain nothing of interest for our analysis. In the remaining 11 epochs the automatic transient detector in AUDACITY will find about 200 events. Sorting out events with low signal level and signal to noise level 84 events were left as possibly useful. These events are listed below with approximate and exact time stamps. The approximate time stamps were used to find the events in high time resolution analysis of the data, when you fill the screen with 10 s of data out of 4 hours, each epoch being analyzed individually.

Pressure test in Ringhals 2 duration 2020-03-31 until 2020-04-03. Acoustic events.

The recording starts at 2020-03-31 at 12:37 (YYYY-MM-DD HH:MM) - calendar time.

Each Epoch (T0XX) is 4h08m30s long. (HH MM SS is epoch time.)

Epoch 7 starts at calendar time 2020-04-01 13:28 the other epochs according to the file copy from the original SD-card, see Figure 13.

200331-T001.WAV	2020-03-31 12:37
200331-T002.WAV	2020-03-31 16:46
200331-T003.WAV	2020-03-31 20:54
200401-T004.WAV	2020-04-01 1:03
№ 200401-T005.WAV	2020-04-01 5:11
№ 200401-T006.WAV	2020-04-01 9:20
№ 200401-T007.WAV	2020-04-01 13:28
№ 200401-T008.WAV	2020-04-01 17:37
№ 200401-T009.WAV	2020-04-01 21:45
№ 200402-T010.WAV	2020-04-02 1:54
200402-T011.WAV	2020-04-02 6:02
200402-T012.WAV	2020-04-02 10:11
№ 200402-T013.WAV	2020-04-02 14:19
№ 200402-T014.WAV	2020-04-02 18:28
№ 200402-T015.WAV	2020-04-02 22:36
№ 200403-T016.WAV	2020-04-03 2:45
200403-T017.WAV	2020-04-03 6:53
№ 200403-T018.WAV	2020-04-03 11:02
№ 200403-T019.WAV	2020-04-03 15:10
№ 200403-T020.WAV	2020-04-03 19:19

Figure 13: Start calendar time for each epoch in the recording.



EXTRACTED EVENTS

(ID, Approximate time in epoch, exact time in epoch, Comment)

The classification in events of different strength is subjective, but the levels can be calibrated with a known source, because the recording levels are known.

Very strong events

- 1, T007, 2h00m40s, 2h00m39.663s, cal.time 2020-04-01 kl 13:28 + 2h00m39.663s
- 2, T007, 2h36m10s, 2h36m06.240s
- 3, T008, 3h13m06s, 3h13m05.963s

Strong events

- 4, T007, 1h15m38s, 1h15m55.942s
- 5, T007, 1h18m45s, 1h18m41.968s
- 6, T007, 1h26m32s, 1h26m33.391s
- 7, T007, 1h56m31s, 1h56m35.783s
- 8, T007, 1h58m17s, 1h58m28.950s
- 9, T007, 2h23m49s, 2h23m49.753s
- 10, T007, 3h09m16s, 3h09m10.362s
- 11, T007, 3h11m39s, 3h11m37.636s
- 12, T007, 3h16m02s, 3h15m39.299s
- 13, T008, 1h35m02s, 1h34m56.478s
- 14, T008, 2h01m18s, 2h01m16.355s
- 15, T017, 0h52m18s, -

Weaker events

- 16, T007, 0h58m25s, 0h58m26.538s, 20 s complex event
- 17, T007, 0h59m34s, 0h59m41.649s
- 18, T007, 1h22m17s, 1h22m18.762s
- 19, T007, 1h40m26s, 1h40m21.819s
- 20, T007, 2h20m04s, 2h20m04.046s
- 21, T007, 2h26m25s, 2h26m27.561s
- 22, T007, 3h17m53s, 3h17m47.275s
- 23, T008, 3h46m37s, 3h46m32.726s
- 24, T014, 3h06m22s, 3h06m20.832s, like a sigh

Weak events

- 25, T007, 1h02m03s, 1h02m7.674s
- 26, T007, 1h09m19s, 1h09m18.555s
- 27, T007, 1h29m02s, 1h28m54.689s



- 28, T007, 1h36m43s, 1h36m39.646s
- 29, T007, 1h39m43s, 1h39m44.582s
- 30, T007, 1h43m09s, 1h43m04.329s
- 31, T007, 1h48m07s, 1h48m22.243s
- 32, T007, 1h51m39s, 1h51m37.194s
- 33, T007, 2h04m19s, 2h04m23.206s
- 34, T007, 2h05m58s, 2h05m54.475s
- 35, T007, 2h13m02s, 2h12m56.088s
- 36, T007, 2h21m26s, 2h21m21.345s
- 37, T007, 2h22m47s, 2h22m45.205s
- 38, T007, 2h34m36s, 2h34m38.049s
- 39, T007, 2h42m05s, 2h42m03.898s
- 40, T007, 2h42m48s, 2h42m46.993s
- 41, T007, 2h43m26s, 2h43m35.590s
- 42, T007, 2h58m41s, 2h38m43.036s
- 43, T007, 3h01m10s, 3h01m12.816s
- 44, T007, 3h13m56s, 3h14m05.243s
- 45, T007, 3h23m35s, 3h23m32.645s
- 46, T007, 3h26m48s, 3h26m52.541s
- 47, T007, 3h34m29s, 3h34m25.990s
- 48, T007, 3h35m37s, 3h35m52.555s
- 49, T007, 3h47m52s, 3h47m47.075s
- 50, T007, 3h58m08, 3h58m07.538s
- 51, T008, 0h13m54s, 0h13m57.299s
- 52, T008, 0h29m53s, 0h29m51.005s
- 53, T008, 0h42m45s, 0h42m41.989s
- 54, T008, 1h11m23s, 1h11m18.544s
- 55, T008, 1h30m54s, 1h30m59.421s
- 56, T008, 1h53m19s, 1h53m12.717s
- 57, T008, 1h56m19s, 1h56m17.634s
- 58, T008, 2h28m23s, 2h28m23.102s
- 59, T008, 2h59m56s, 2h59m53.474s
- 60, T008, 3h20m22s, 3h20m25.519s
- 61, T011, 1h56m38s, 1h56m40.475s
- 62, T011, 2h02m51s, 2h02m55.536s
- 63, T011, 2h27m08s, 2h27m04.136s
- 64, T011, 3h17m40s, 3h17m35.400s
- 65, T011, 3h44m08s, 3h44m03.201s



```
66, T011, 3h45m35s, 3h45m28.297s
67, T012, 0h08m37s, 0h08m34.886s
68, T012, 0h12m08s, 0h12m12.035s
69, T012, 1h01m32s, 1h01m34.048s
70, T012, 1h10m09s, 1h10m05.095s
71, T012, 1h44m48s, 1h44m46.962s
72, T012, 2h00m34s, 2h00m38.516s
73, T012, 2h39m35s, 2h39m30.187s
74, T012, 3h46m37s, 3h46m40.015s
75, T013, 0h32m47s, 0h33m51.751s
76, T013, 1h45m23s, 1h44m19.244s
77, T014, 1h04m01s, 1h03m56.267s
78, T017, 4h00m32s, 4h00m36.068s
79, T018, 0h12m15s, 0h12m6.545s
80, T018, 0h35m11s, 0h35m09.810s
81, T018, 0h59m27s, 0h59m28.205s
82, T018, 1h13m59s, 1h13m55.862s
83, T018, 1h27m53s, 1h27m56.684s
84, T018, 1h43m58s, 1h43m57.883s
```

RATE OF EVENTS IN EACH RELEVANT EPOCH

```
Epoch 7: 2020-04-01 13:28:00 44 events
Epoch 8: 2020-04-01 17:37 14 events

Epoch 11: 2020-04-02 06:02 6 events
Epoch 12: 2020-04-02 10:11 8 events
Epoch 13: 2020-04-02 14:19 2 events
Epoch 14: 2020-04-02 18:28 2 events

Epoch 17: 2020-04-03 06:53 2 events
Epoch 18: 2020-04-03 11:02 6 events
```

With some fantasy it is possible to distinguish three periods in the rate of events related to the nature of the mechanics behind the emissions. The first, Epoch 7-8, could be a *brittle* failure, the last, Epoch 17-18, a slow failure etc. The brittle period would be strong events with a short duration imagined to be the development of a brittle failure associated with the load level. The later period would be associated with *creep*, the slow deformation under pressure, that will eventually result in a less explosive fracture. The history of such an event is most likely extended in time compared to a brittle failure.

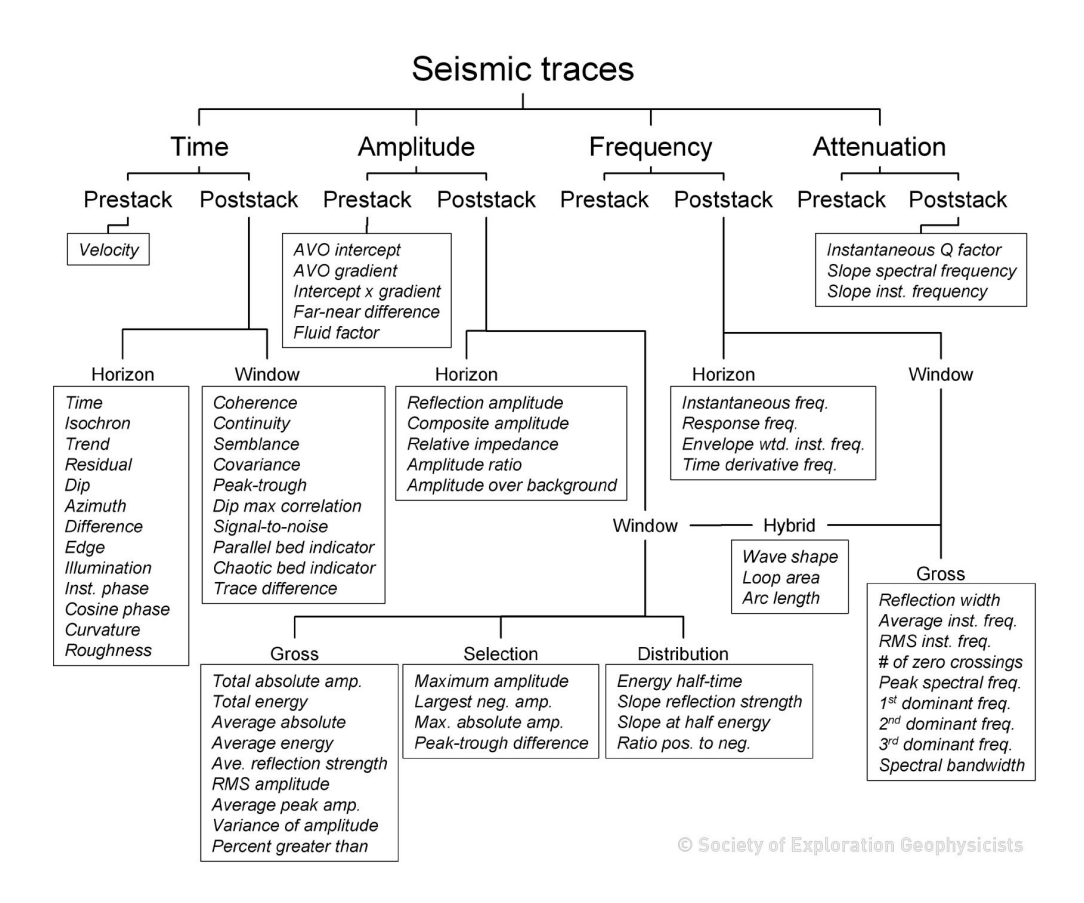
Peter Jonsson at Teknisk Geologi LTH has suggested that the science of seismology may have something to contribute regarding the interpretation of the mechanics of



events. A difference is that the airborne emissions contain no shear wave information as structure borne emissions do. This is because air, like water, cannot support shear waves. According to Björn Lund, seismologist, with special interest in source mechanics, at Uppsala universitet, most earthquake sources are of shearing nature, although they emit both shear (S) and compression (P) waves. An exception were the identification of nuclear bomb test for which the Swedish seismological network was developed. They generate P-waves at the source, but as a consequence of these also S-waves are generated. An earthquake can be classified according to the frequency content. There is e.g. a characteristic upper *corner frequency*, limiting the bandwidth of the frequency plateau, generated by the rupture.

Seismic attributes are used in reflection seismology to enhance the information content in received signals. There are now more than 200 such attributes in use in reflection seismics. Many of these have with the 2-D and 3-D nature of reflections seismic survey results to do. Due to the difference in data collection method only some of them may be useful in enhancement of information in acoustically detected emissions during pressure tests. The most common type of attribute is amplitude, which has already been used in the categorization of the emissions. Another attribute that could be of interest to study is instantaneous frequency, strongly related to the local curvature of the received signal.

Table 1. Some attributes used in reflection seismics.
(https://petrowiki.org/Seismic_attributes_for_reservoir_studies)



Seismic data collection is made with hundreds of geophones distributed along a line or a 2-D grid. In order to improve the data quality a process called stacking is performed. It is a kind of averaging of many signal traces and it enhances weak echoes. This is the reason for the headings in Table 1 labelled pre-stack and poststack. A more or less continuous reflector is labelled a horizon, often representing the interface between two different geological layers. A window could be many things, like a processed part of a signal or more common all the displayed signals, that together show different horizons. The window may be focused on a specific time interval in the reflected signals. All this has little application to acoustic measurements in an NPP, but is discussed for completeness and for indicating the possibility that there may be more to extract from the acoustic signals in the NPP than the arrival times to the different microphones.

Recently a paper (2) from Carnegie Mellon University describes how sound was used in robotic classification in combination with vision and proved to be useful. Sound can e.g. discriminate between an empty and a full beer-can, which vision cannot.

They use a classification scheme based on a Short Time Fast Fourier Transform, image transformation and a neural network to arrive at the classification. An inherent problem with neural networks - artificial intelligence i.e. is that the technique requires a training set. For large and extremely valuable constructions this is simply not possible to get and thus the learning phase of the neural network has to be simulated. Something that renders it less reliable, of course.



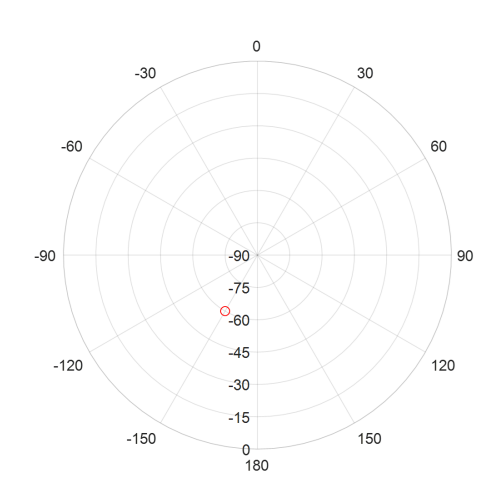
4.2 CALCULATING THE DIRECTION TO THE SOURCE OF EVENTS

The presentation of the result from the direction finding calculations is done in one upper (zenith-direction) and one lower (nadir-direction) hemisphere. Events to the left of the upper microphone array boom are presented with negative azimuth values (0 to - -180 degrees) and events to the right with positive azimuth values 0 - +180 degrees). Zero azimuth is in the direction of microphone 1 in the upper boom. The elevation is presented as a positive angle 0-90 degrees in the upper hemisphere and as negative values in the lower hemisphere. This convention means that azimuth values -180 degrees is the same azimuth as +180 degrees. [This is a property of circles also on an Earth globe. As known already by Christopher Columbus if you go far enough to the west you end up in the west (unless you discover America)]. See Figure 14.

Northern hemisphere

Azimuth: -150 deg Elevation: 60 deg

Southern hemisphere



Azimuth: -150 deg Elevation: -60 deg

Figure 14: Graphic presentation of the angles convention in this report. The diagrams do not render any distances, only angles. Picture by Karim Haddad, Brüel&Kjaer Denmark.

Since the result only present directions it does not matter that the microphone array was placed in an eccentric position in the containment.

The equatorial plane, for which the elevation is zero degrees, is the plane imagined between the microphone booms in the array, i.e. perhaps 2 meters above the top of the cantilever it rests on.

Most events occur in the upper hemisphere. Among these some direction calculations are more reliable than others. The most reliable event directions are presented in Figure 15, the more questionable in Figure 16.



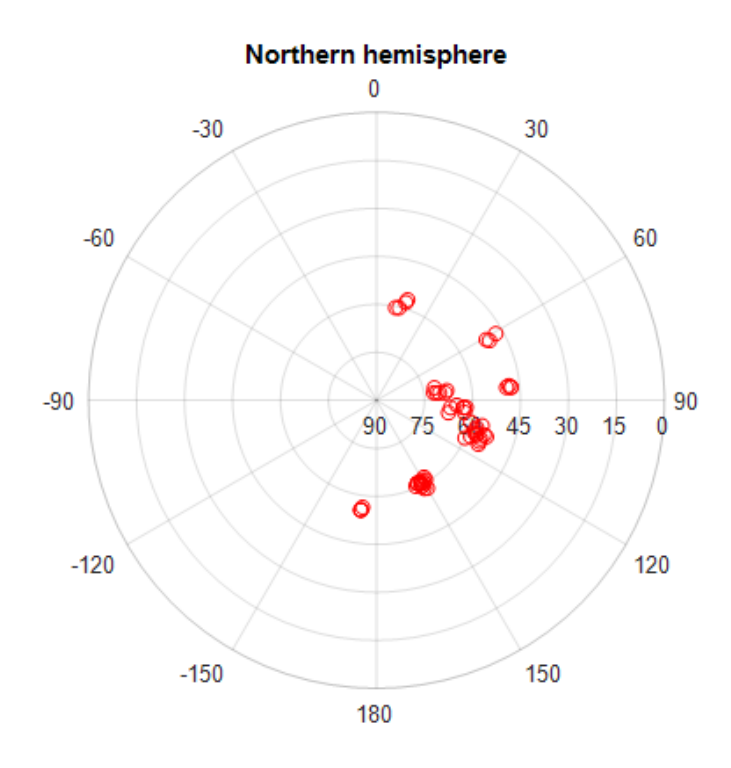


Figure 15: The most reliable direction calculations occur in the upper, northern hemisphere. As can be seen they are located mainly to the right of the upper microphone array boom. Diagram by Karim Haddad, Brüel&Kjaer.

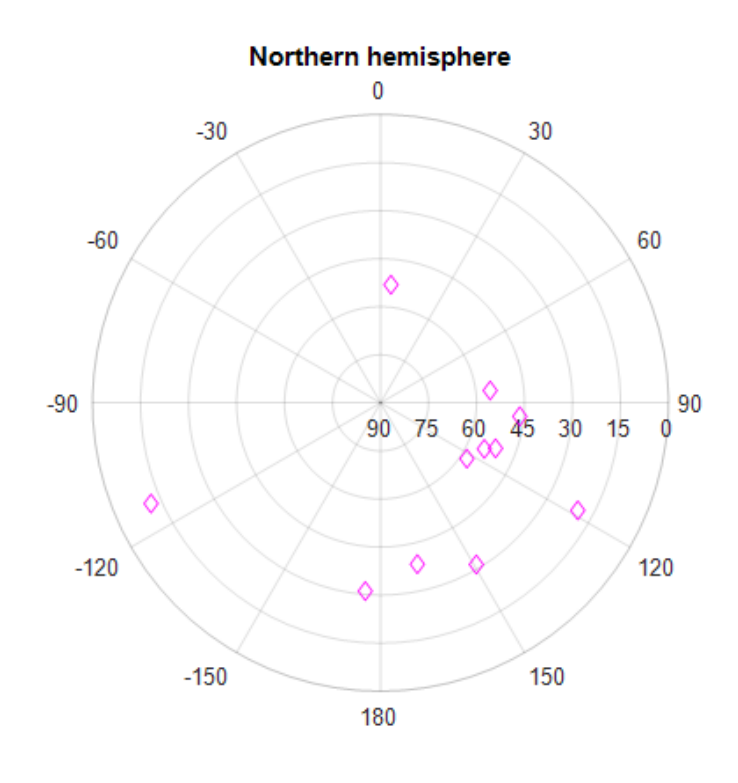
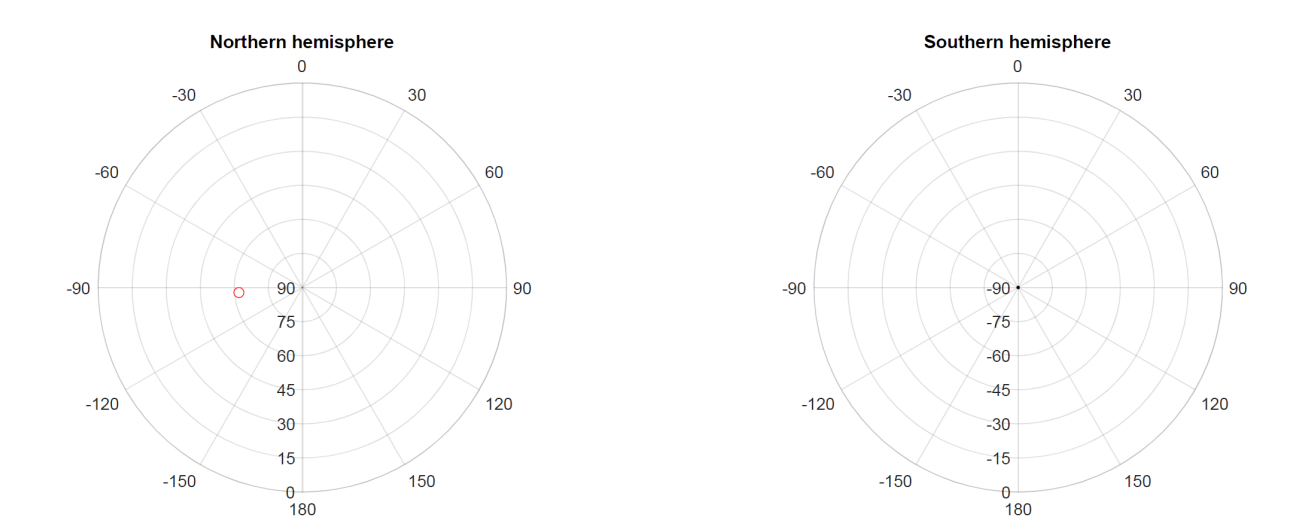


Figure 16: The more questionable direction calculations. Diagram by Karim Haddad, Brüel&Kjaer. For these, there were no obvious onsets.



For all individual events the results are presented in the subsequent pages according to the convention in Figure 17 below.



Elevation: 61.9 degrees - Azimuth: -94.5 degrees

Figure 17: The convention for presenting the direction to all the individual events. When there is doubt about the confidence this is indicated in red text. Diagram by Karim Haddad, Brüel&Kjaer.

Below follows part 2 of the report presenting the calculations of directions to the extracted events. It is written by Karim Haddad, Brüel & Kjær Sound & Vibration Measurement A/S $\,$



5 Introduction to direction finding

When a construction under pressure undergoes irreversible structural modifications, elastic waves are generated in the structure that can cause acoustic radiation in the vicinity. It is therefore useful to track and locate these acoustic events, to monitor the structural modifications of a construction.

An acoustic event generated by structural changes in a building are generally transient in nature, with a relative short duration, like a gunshot sound. For a couple of microphones with known distance between them, there is a delay between the instant when the closest microphone detects the event, and the instant when the second one detects it. This delay is directly linked to the direction of the acoustic event, relatively to the axis joining the 2 microphones position. A minimum of 4 non-coplanar microphones are needed to localise an acoustic source in 3D space.

In this report, we estimate the directions of acoustic events, using recordings from a 4-microphones array designed and developed by Doc. Peter Ulriksen from Lund University.

In total we get 84 recordings, most of them containing a single acoustic event. For the majority of them, the onset of the events (real start of the event) is obvious. For a few of them, the onset was less obvious, and therefore the results are less to be trusted. We show here 75 localisation results. From these events, 59 contains obvious onsets, the 16 remaining are more difficult.

In the first part, we describe the microphone array (briefly since this is explained by Doc. Peter Ulriksen in a separate report) and the convention for the expressing the location of the events. In a second part, the types of signals are detailed, as well as the assumptions taken for the analysis. Finally, we will report the results for the 75 analysed events.



6 Microphone array and convention

The microphone array consists of 4 microphones. The layout is presented in the figure below.

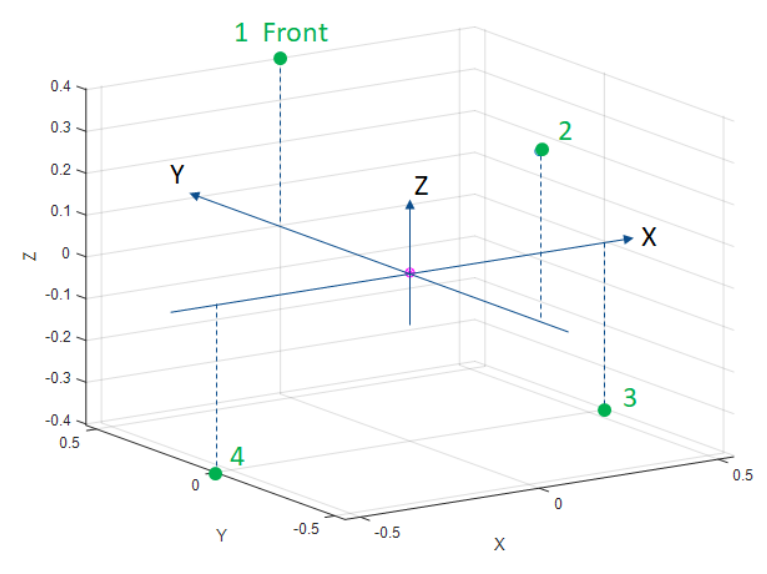


Figure 18: Layout of the 4-microphone array

The distance between microphones 1 and 2, 3 and 4 is 1.086 meters (m). The other distances between microphone pairs (1 and 3, 1 and 4...) are 1.1133 m.

To describe the location of an acoustic source, we use spherical coordinates: the azimuth and the elevation. The convention for these coordinates is given below.

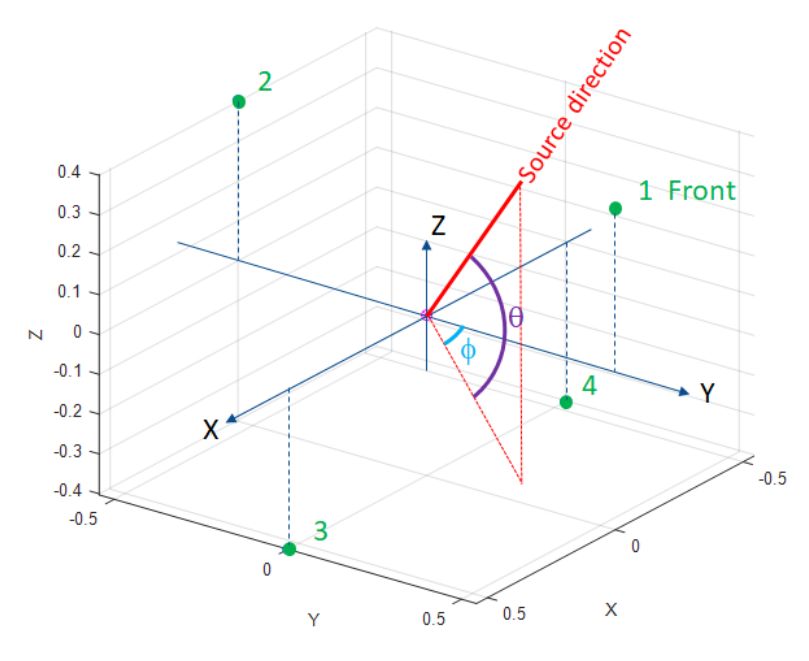


Figure 19: Spherical coordinates for the location of an acoustic event



The source direction is provided by the azimuth ϕ in the range -180 to +180 degrees and the elevation θ in the range -90 to +90 degrees. The azimuth of the source is at 0 degree when it faces the microphone 1 (assumed as the Front of the array). The elevation of the source is at 0 degree when it is in the horizontal plane of the array.

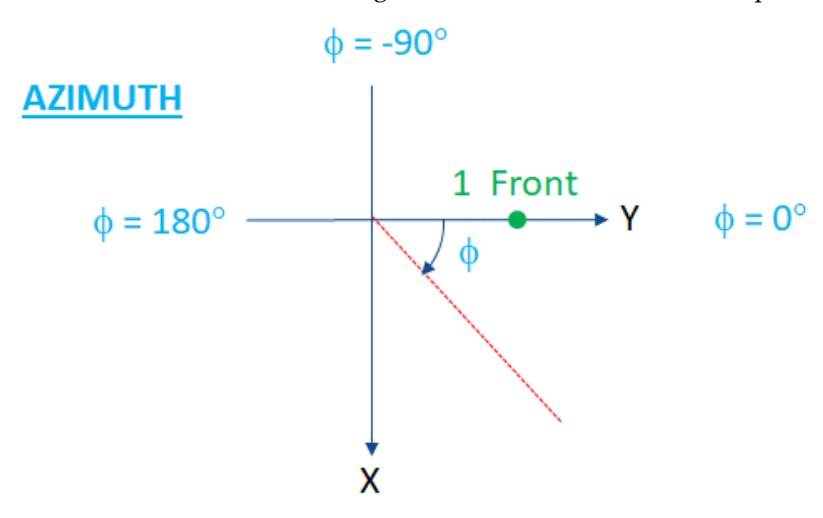


Figure 20: Convention for the azimuth angle

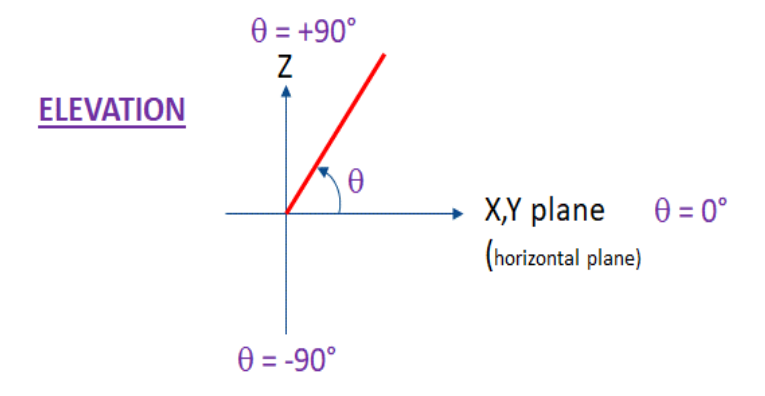
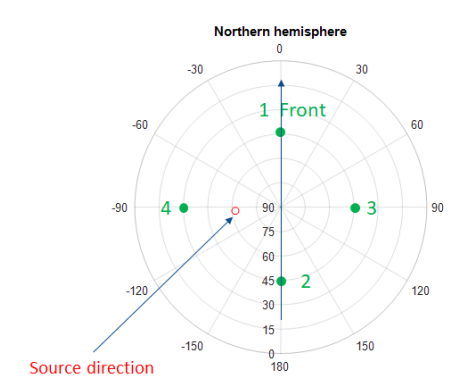


Figure 21: Convention for the elevation angle

To display the localisation of each event in the document, we consider polar plots, one for each hemisphere. The 'Northern hemisphere' shows acoustic sources for elevations between 0 and 90 degrees, therefore in the upper part of the array. The 'Southern hemisphere' indicates sources for elevations between -90 and 0 degrees, so the bottom part of the array. The angles in the polar plot are the azimuth, the radius of the polar plot reports the elevation of a source.





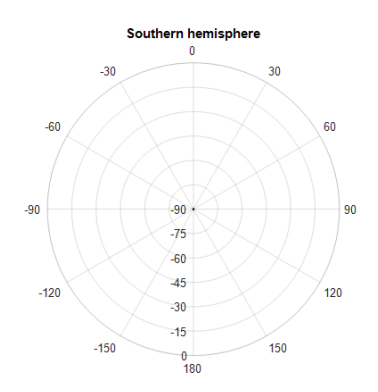


Figure 22: Presentation of the acoustic event direction. For this example, the source direction is 62 degrees in elevation and -94.5 degrees in azimuth



7 Processing of the microphone signals

7.1 THE SIGNALS

The acoustic signals generated by events are transient. The acoustic events reach each microphone at different timestamps, depending on the source position. For most cases, the events are easy to spot in the recordings, as illustrated on the picture below. For the test of the figure, the event reaches first the microphone 2, then very shortly after microphone 1, the microphone 3 and then 4. It says then that roughly the source is almost at 90 degrees of the line joining the microphone 1 and 2 (since the associated wave-front reach both microphones at almost the same time), and in the direction of microphone 3, compared to microphone 4. From this quick analysis, it is obvious that the delay estimation between sensors is key in the processing for the localisation of the acoustic events. This process can be automated using algorithms such as explained below. However, we need to select a proper time window that extracts the start of the event. For the case of the signal below, the start of the event in the recording is clear.

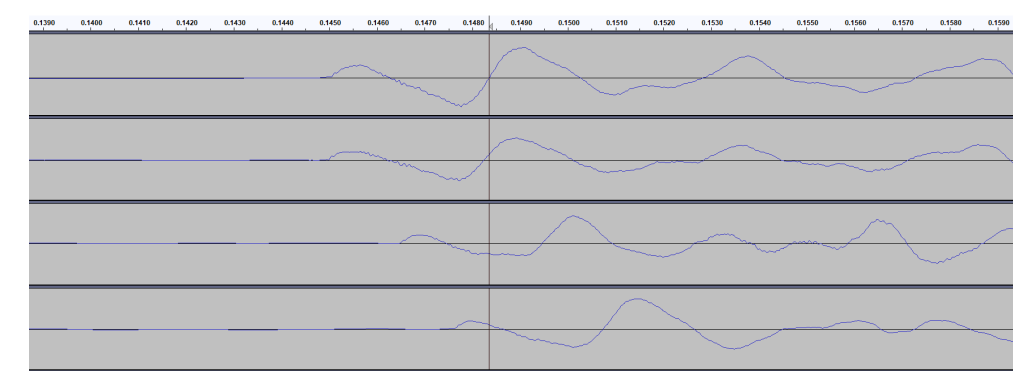


Figure 23: recordings from the 4 microphones (mic. 1 at top, mic. 4 at the bottom), test 1

But there are a few tests, where the real start of the event is not obvious, as illustrated on the example below.

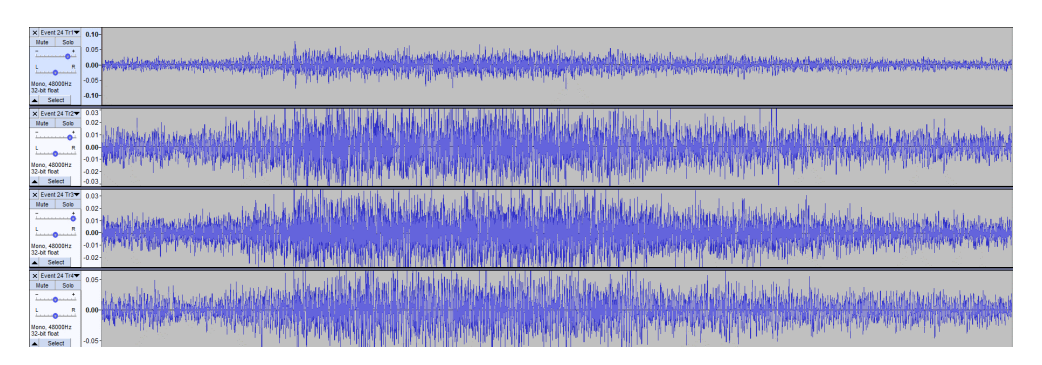


Figure 24: recordings from the 4 microphones (mic. 1 at top, mic. 4 at the bottom), test 24



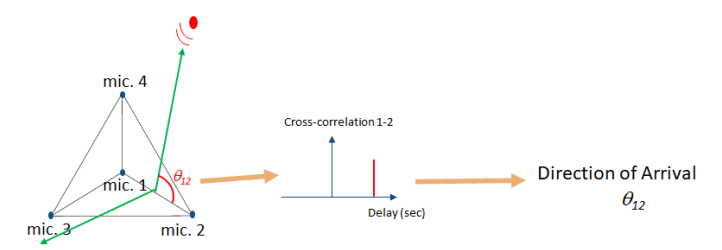
The main reason for these noisy signals is due to previous events that are still reverberating in the enclosure.

For these cases, it is difficult to select a proper time window that contains the onset of the event signal. If the onset is not selected, then the localised source is probably due to a reflection, from another surface, of the acoustic event. Therefore, the localisation error could be large.

In total we have processed 75 events. 59 events present obvious onset. For 16 events, the localisation error is probably large.

7.2 ARRAY PROCESSING

The principle of the array processing is exposed below.



- From all the pairs 1-2, 1-3, 1-4, 2-3, 2-4, 3-4, we get a set of directions θ_{12} , θ_{13} , θ_{14} , θ_{23} , θ_{24} , θ_{34}
- The fusion of all these angles provides an estimation of the source position.

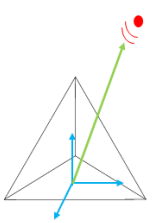


Figure 25: Principle of array processing to localise an acoustic event

For each microphone pair, we estimate the delay between signals using cross-correlations. This delay is directly link to a direction of a source, relative to the axis joining the 2 microphones of the pair. Fusing all the directions estimated for each pair, we obtain a localisation in the 3D space.

7.3 ASSUMPTIONS

The distances between the microphones and the surfaces in the building are much larger than the size of the array. It is then suitable to use a plane wave model. Based on this assumption, it is not possible to estimate the range of the source.

If three more microphones in a line are used the curvature of the wave-front and hence the source distance, can be calculated, the source being located at origo of the curvature.



The processing depends on the speed of the sound, which is based on the temperature in the building, see below. It is assumed that the temperature is constant, at 26.6° Celsius for all tests, and the speed of sound is then 347 m/s.



Figure 26: Temperature evolution during pressurisation.



8 Results

8.1 OVERALL RESULTS

Very few events are in the bottom hemisphere, only those with probably large errors. The most reliable results are in the top hemisphere. The following polar plot shows the localisation of the 59 events with obvious onset.

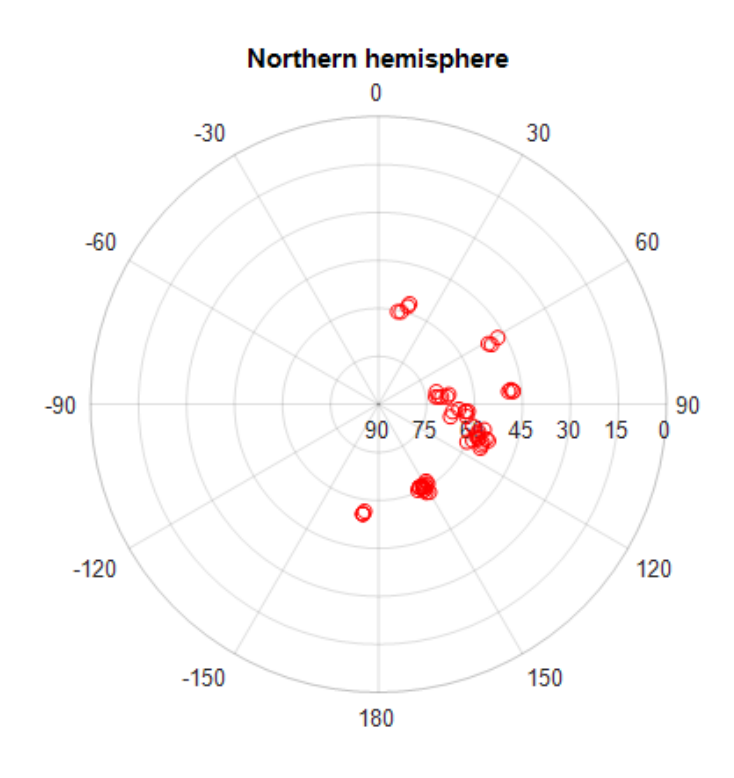


Figure 27: Localisation of acoustic events with obvious onsets

Most of these events are localised for positive azimuths, so on the right side of the line joining microphone 1 and 2 (see Figure 22). The elevations of the localised events are in the range 45 to 75 degrees.

We show also below the positions of the events that have higher errors.



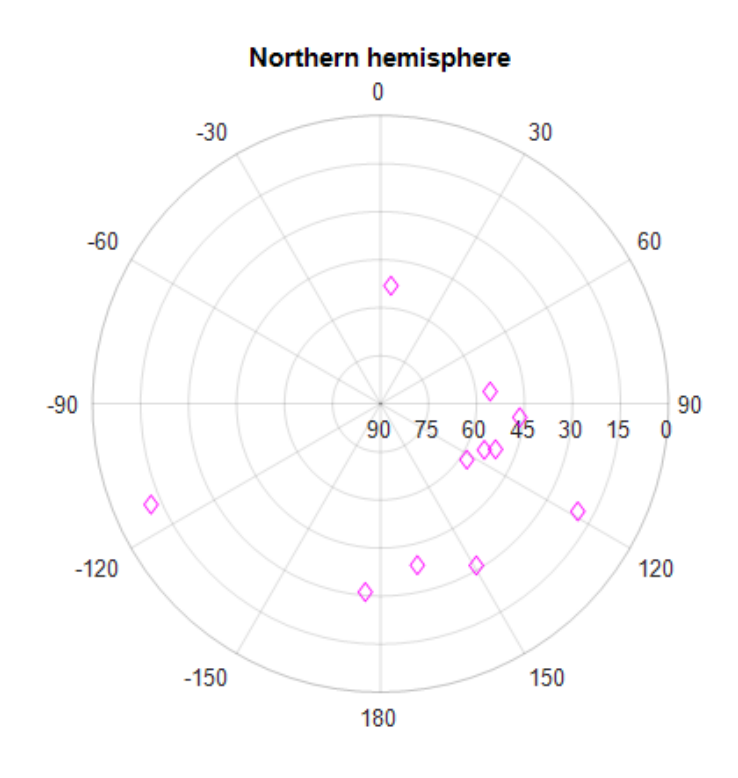
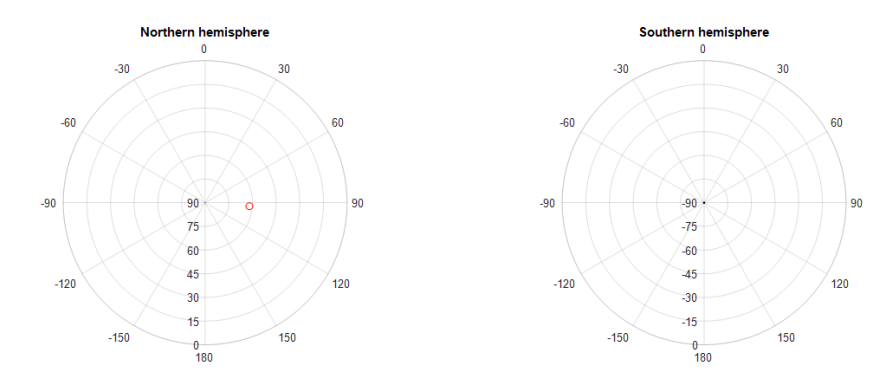


Figure 28: Localisation of acoustic events with no obvious onsets Individual results

8.2 INDIVIDUAL RESULTS

We show below an example of the graphic presentation for the first of the 75 analysed events. A complete presentation of all events is contained in Attachment 2 to this report. Each event can be generated either in the upper (northern) hemisphere or in the lower (southern) hemisphere. Thus there are two polar plots for each event. The location of the event is a small red circle.



Elevation: 61.9 degrees - Azimuth: +94.5 degrees

Figure 29: Test 1



9 Conclusions

This study shows that a microphone array is a suitable technique to *localise the source* of acoustic emissions generated in the dome of a pressurised nuclear containment. The main condition required being the unobstructed *line-of-sight* between sources and microphones.

The reactor Ringhals 2 has been pressurised, generating a large number of acoustic emissions. The automatic transient detector in the software AUDACITY detected about 200 transients. Out of these 84 were manually selected as feasible for calculations, mainly based on the attribute amplitude. Based on these events, a total of 75 events are analysed in this report. 59 events are localised with high confidence. The localisation of the 16 remaining events are estimated with less confidence. Those that were not analyzed did not produce convergent data.

No events could be identified in the noisy compression/decompression phases, not even when the low sensitivity records were studied in detail.

Most events occurred during the first 8 hours after the compression phase had stopped, but there is also some events in late epochs, just before the decompression phase starts.

Almost all events are located in the upper, northern hemisphere, coincident with the dome in the reactor containment, which has an inside surface mounted liner. Because of that it seems possible to associate the events with pressure induced tensions in the welds or in the bond between the liner and the concrete, supported by studs.

There may be more information to harvest in this kind of transient records, but that has to be referred to another study, with another time scale. This report was produced 6 weeks after the pressure test in Ringhals 2.

These findings should be followed by detailed inspection of the indicated sources of emissions together with personnel at the NPP Ringhals.

Keywords

Acoustic emission – Pressurised building - microphone array – Acoustic source localisation



10 References

- The ACCEPPT publications are not public, but an open summary is given in the following report (1) by Lundqvist, available at the Energiforsk homepage reports.
- (1) LUNDQVIST, P., (2016) "ACCEPPT Aging of concrete and civil structures in nuclear power plants." Energiforskrapport 2016:265
- (2) Gandhi, D., Gupta, A. and Pinto, L., "Swoosh! Rattle! Thump! Actions that sound", Conference paper in Robotics, Science and Systems 2020, Corvallis, Oregon, USA, July 12-16 2020.



Appendix A: Attachment 1 Technical manual (in Swedish)

INSTRUKTION FÖR ATT MONTERA TETRAHEDER OCH STARTA LJUDINSPELNING

Utrustningen anländer som två komponenter: Ett vapenfodral och en grå låda med fyra vidhängande mikrofonkablar.

Vapenfodralet innehåller ett stativ för att hålla uppe tetrahedern, tetrahedern, mikrofonerna, verktyg för att spänna kronmuttrar, nyckel till den grå lådan och en laser som används för att bestämma tetrahederns riktning relativt reaktorinneslutningen.

Den grå lådan innehåller ljudinspelaren ZOOM F8, AC-adapter och ett litiumbatteri. ZOOM F8 kan drivas antingen från 230V via AC-adaptern eller via externt batteri. Den kan också drivas med interna batterier men det är inte aktuellt i detta fallet på grund av den långa inspelningstiden, cirka 5 dygn max.

Montera Tetrahedern

- 1. I vapenfodralet finns ett stativ. Fäll ut foten så att den får största möjliga spridning och drag upp stativet så att toppen kommer i axelhöjd.
- 2. I vapenfodralet finns sex kolfiberstänger. Fyra är likadana, två avviker. En av dessa har ett mässingsrör mitt på och en bit kromtejp vid ena änden. Denna stång skall sitta överst i tetrahedern. Lossa kronmuttern vid kromtejpen. Änden med kromtejpen förs genom hållaren överst på stativet och mässingsröret placeras mitt i hållaren, så att lika långa bitar sticker ut på ömse sidor om hållaren. Spännskruven dras åt.
- 3. I vapenfodralet finns fyra rostfria mikrofonhållare som alla ser likadana ut. Lossa kronmuttrarna från den på stativet monterade kolfiberstången och montera en rostfri hållare i varje ände av kolfiberstången.
- 4. Montera de fyra likadana kolfiberstängerna, två i varje hållare och drag åt kronmuttrarna för hand.
- 5. Drag upp stativet så att det blir så högt det kan bli.
- 6. Montera nu de två återstående rostfria hållarna på de fyra fria ändarna av kolfiberstängerna.
- 7. Montera den återstående kolfiberstången, den med maskeringstejp mittpå i de nedersta hållarna. Tejpa fast den understa stången så att dess markerade mitt kommer mitt på stativets vertikala stång.
- 8. I vapenfodralet finns en laser som ser ut som en hagelpatron. Skruva ut den bakre mässingsdelen och avlägsna tejpen. När mässingsdelen skruvas i igen tänds lasern. Lägg lasern i blixtinfattningen längst upp på stativet. Lasern kommer nu att peka i samma riktning som den översta kolfiberstången. Notera var i reaktorinneslutningen ljuspunkten träffar. Stativet bör stå mitt på golvet i inneslutningen om det är möjligt.
- 9. Montera mikrofonerna i de rostfria hållarna. De skall sticka ut c:a 5 mm så att hela gallret blir synligt, se figur. Spänn fast med nylonskruvarna.



Mikrofonkablarna är de svarta kablarna som kommer ut från den grå lådan. De är numrerade 1-4 och skall anslutas enligt följande schema:

- a. Den mikrofon som sitter överst i den riktningen lasern pekat är mikrofon 1 och ansluts med kabel 1.
- b. Den mikrofon som sitter i andra änden på översta stången är nummer 2 och ansluts med kabel 2.
- c. Den mikrofon som sitter nederst till höger sett mot laserpunkten är mikrofon 3, ansluts med kabel 3.
- d. Den mikrofon som sitter nederst till vänster sett mot laserpunkten är mikrofon 4 och ansluts med kabel 4.
- e. Mikrofon 1 är därför FRÄMRE, mikrofon 2 är BAKRE, mikrofon 3 är HÖGER och mikrofon 4 är VÄNSTER.
- f. Mikrofonerna 1 och 2 är på samma sätt ÖVRE medan mikrofonerna 3 och 4 är UNDRE.
- 10. Tejpa fast kablarna till stativet med eltejp på jämna mellanrum hela vägen ned till underlaget.

Grå lådan

Ljudinspelaren ZOOM F8 är förinställd så att den skall spela in 4 kanaler 1-4 med nivåkontrollen rakt upp, kl. 12, medan kanalerna 5-8 spelar in samma ljud, men med nivåkontrollerna rakt åt vänster, kl. 9. Detta görs för att både starka och svaga ljud skall kunna framträda. Dessa inspelningar dubbleras så att en kopia hamnar på ett 512 GB SD-kort och en kopia på ett annat 512 GB SD-kort. Avsikten är att ett SD-kort stannar på Ringhals, det andra skickas till LTH. Med valda parametrar 24 bit digitalisering och 48 kSa/s räcker 512 GB till 123 timmars inspelning. SD-korten sitter upptill bakom två små luckor på ZOOM F8 vänstra gavel. På samma gavel sitter mikrofoningångarna 1-4 som är anslutna och längst upp till vänster på gaveln finns kontakten för anslutning av extern DC-försörjning.

AC-adaptern är nedstucken i nätkontakten i grå lådan. Den ansluts till ZOOM F8 via kontakt baktill på ljudinspelaren.

Litiumbatteriet har en rödsvart kabel med monterad Highrose-kontakt som passar den lilla runda kontakten på ljudinspelarens vänstra gavel, där den sitter längst upp till vänster.

Kabelgenomföringarna är tätade liksom lådans lock, men inte hermetiskt. Detta kunde leda till bekymmer när lådan skall öppnas, eftersom det då kan råda övertryck i lådan. Därför är en av kabelgenomföringarna ihålig med en tops-pinne instucken i hålet. Genom detta arrangemang hålls lådans inre vid samma tryck som omgivningens utan att partiklar kan tränga in.

Ljudinspelaren

- 1. Tryck på den lilla kontakten längst ner till höger på ljudinspelarens front. Displayen skall tändas.
- 2. Tryck på den stora kontakten med röd punkt. Alla röda lysdioder 1-8 skall tändas och ljudinspelningen är påbörjad.
- 3. Stäng locket på grå lådan och lås med nyckeln som finns i vapenfodralet.



- 4. Mät
- 5. Öppna lådan och tryck på stopptangenten (fyrkant). Tryck på strömbrytaren längst ner till höger. Ta ut SD-korten. Klart.



Så här skall mikrofonerna monteras. Spänn fast för hand med nylonskruvarna.

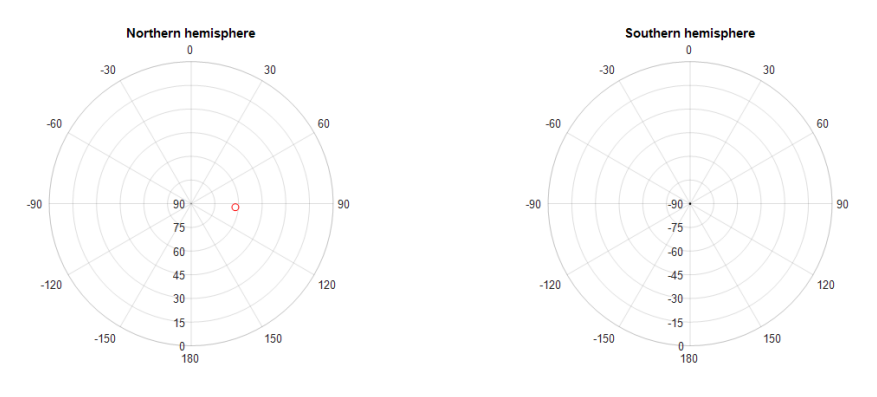


Mittmarkering på översta kolfiberstången (mässingsrör) och laser lagd i blixtsko.



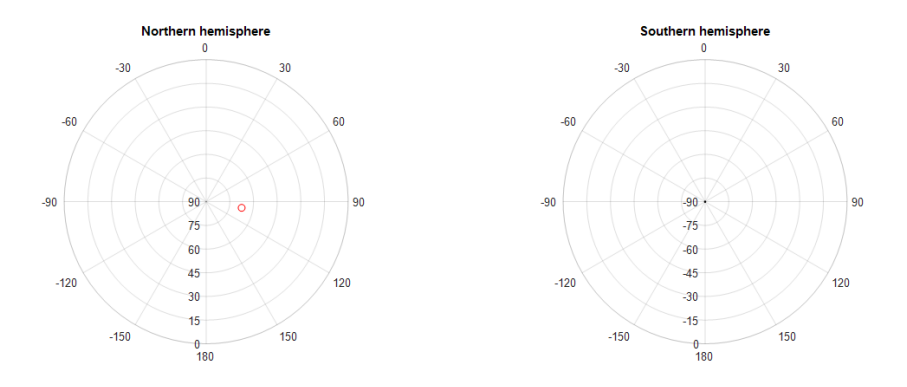
Appendix B: Attachment 2 Individual Event Location

This is a continuation of Chapter 8.2. As mentioned previously each event can be generated either in the upper (northern) hemisphere or in the lower (southern) hemisphere. Thus there are two polar plots for each event. The location of the event is a small red circle. An event can only reside in one hemisphere.



Elevation: 61.9 degrees - Azimuth: +94.5 degrees

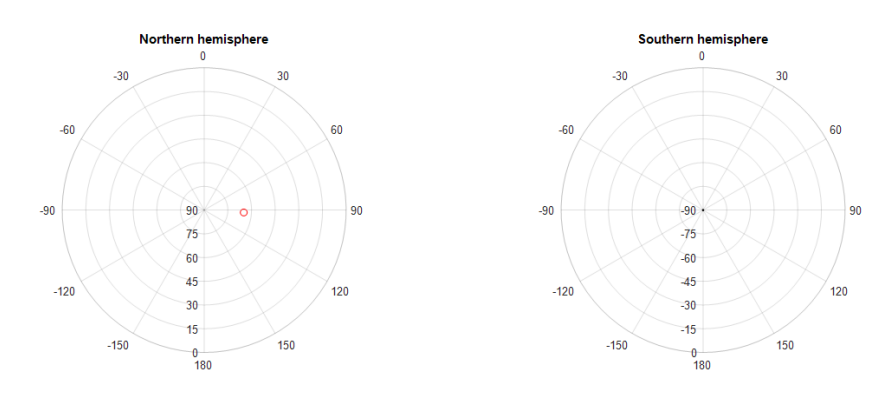
Figure 29:Test 1



Elevation: 67.2 degrees - Azimuth: +99.8 degrees

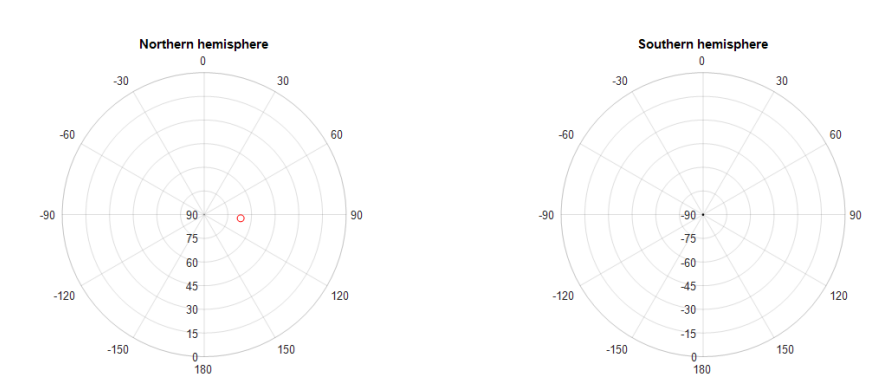
Figure 30: Test 2





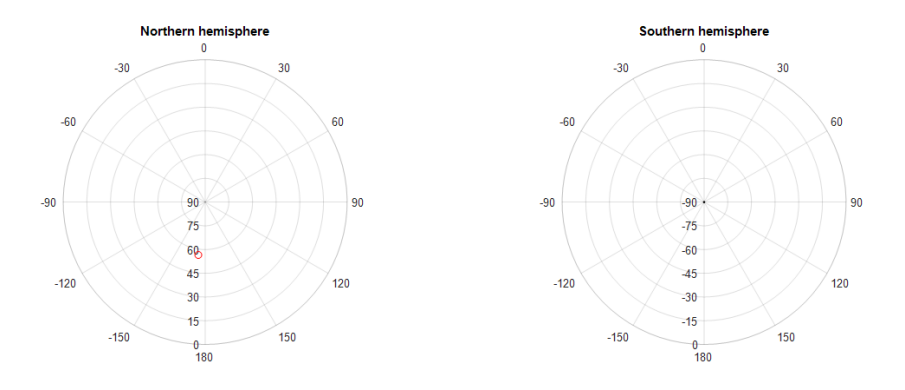
Elevation: 64.8 degrees - Azimuth: +93.4 degrees

Figure 31: Test 3



Elevation: 66.8 degrees - Azimuth: +95.7 degrees

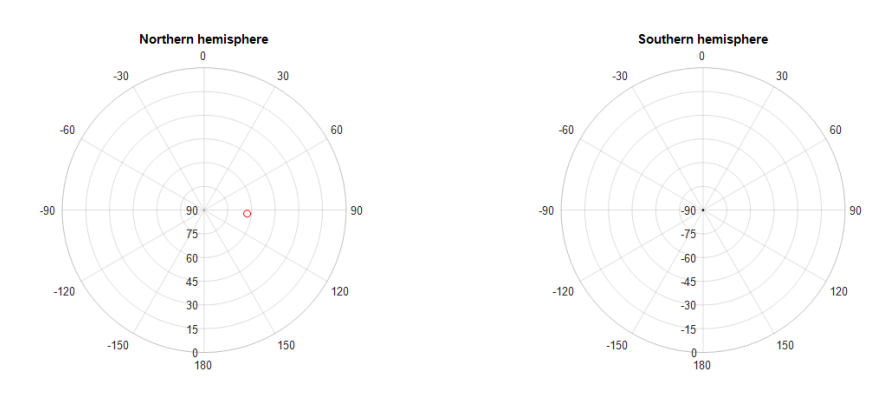
Figure 32: Test 4



Elevation: 56.3 degrees - Azimuth: -172.6 degrees

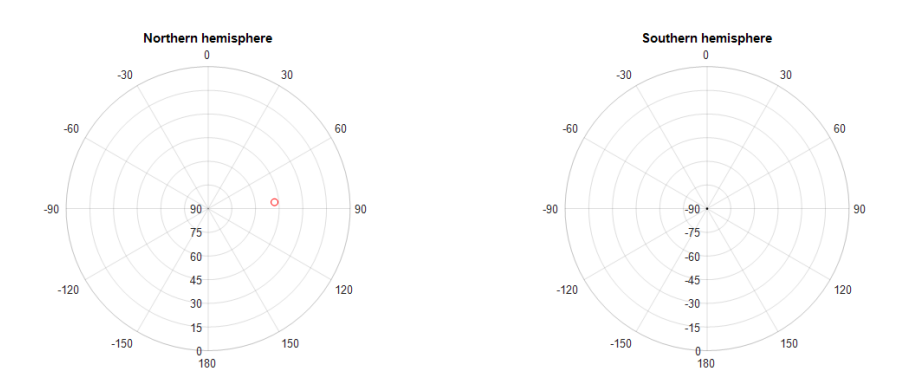
Figure 33: Test 5





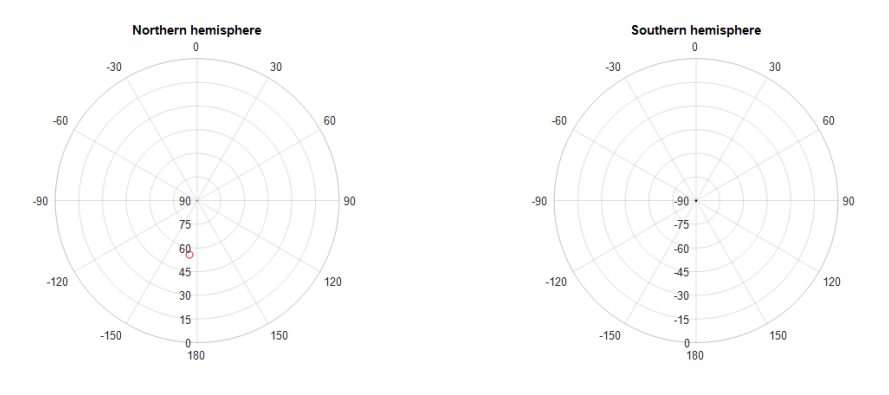
Elevation: 62.7 degrees - Azimuth: +94.7 degrees

Figure 34: Test 6



Elevation: 47.8 degrees - Azimuth: +84.4 degrees

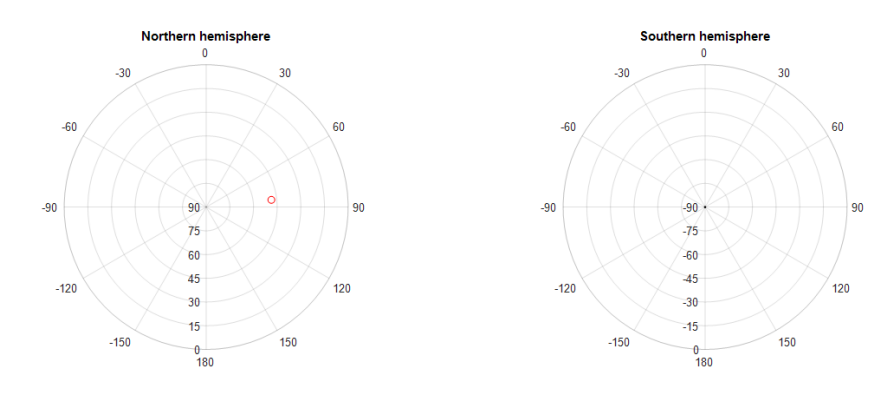
Figure 35: Test 7



Elevation: 55.4 degrees - Azimuth: -171.9 degrees

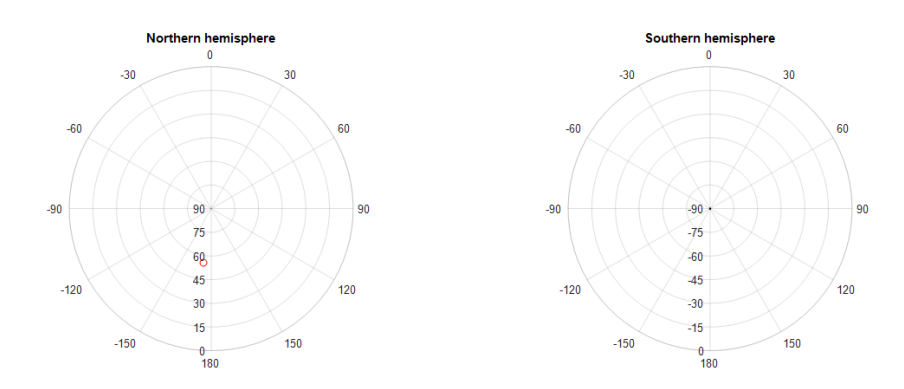
Figure 36: Test 8





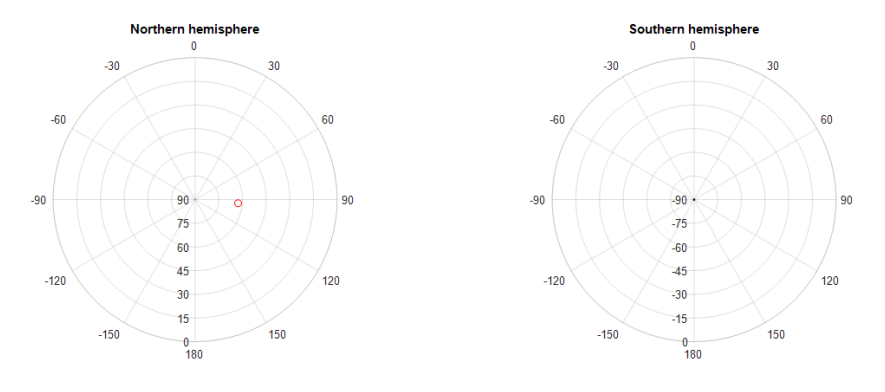
Elevation: 48.4 degrees - Azimuth: +83.7 degrees

Figure 37: Test 9



Elevation: 55.4 degrees - Azimuth: -171.9 degrees

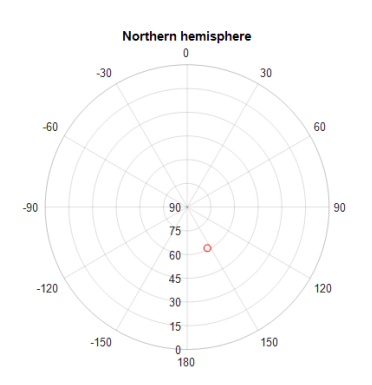
Figure 38: Test 10

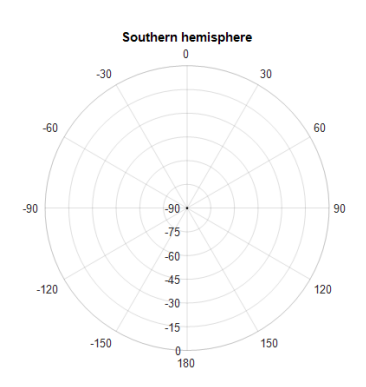


Elevation: 62.7 degrees - Azimuth: +94.7 degrees

Figure 39: Test 11

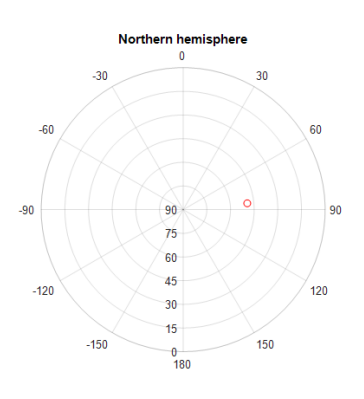


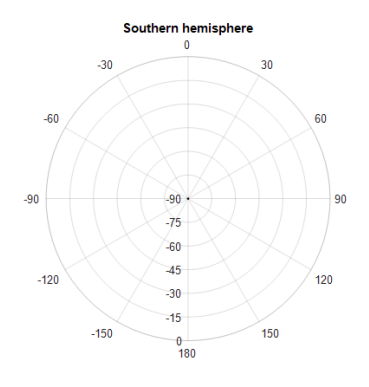




Elevation: 61.1 degrees - Azimuth: +153.7 degrees

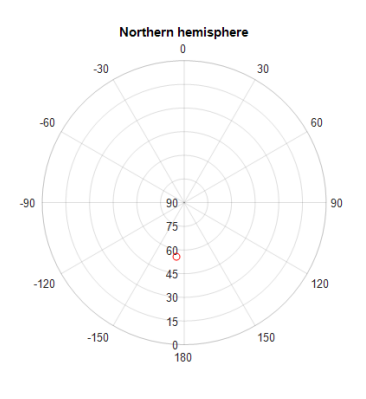
Figure 40: Test 12

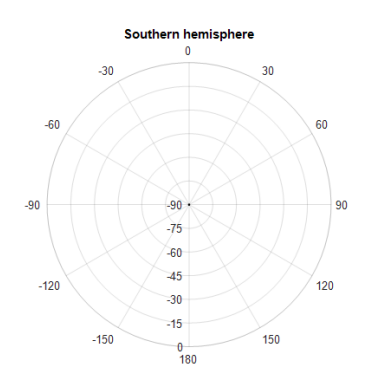




Elevation: 49.2 degrees - Azimuth: +84.3 degrees

Figure 41: Test 13

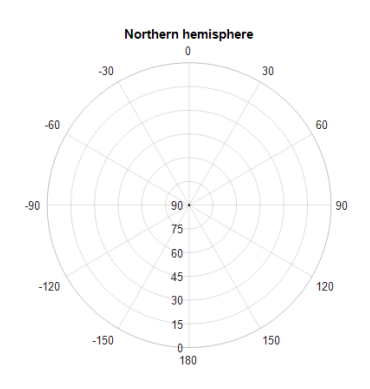


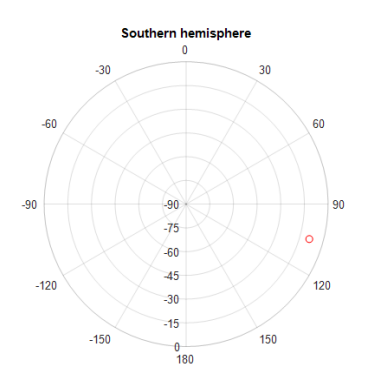


Elevation: 55.4 degrees - Azimuth: -171.9 degrees

Figure 42: Test 14



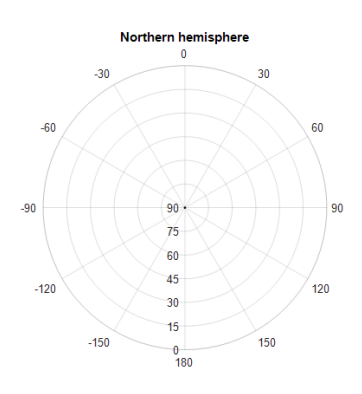


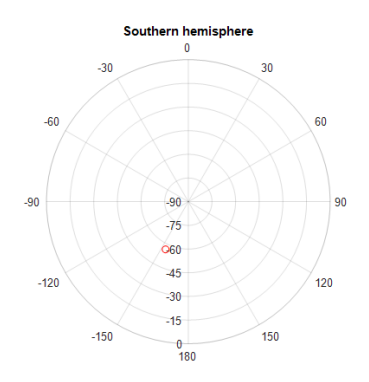


Elevation: -8.9 degrees - Azimuth: +105.7 degrees

<u>Note</u>: Different nature of sound, compare to previous tests – Error localisation could be high in this case

Figure 43: Test 15

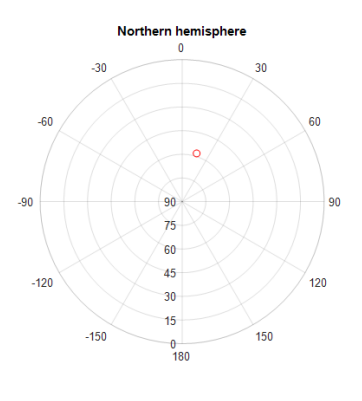


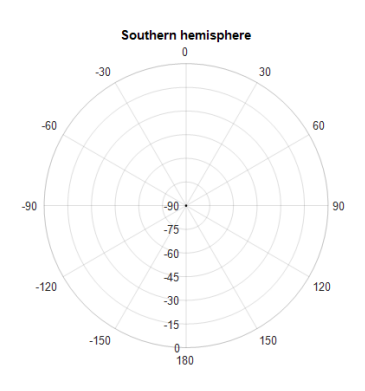


Elevation: -56.5 degrees - Azimuth: -154.5 degrees

<u>Note</u>: mutiple sounds in the recording, considered the loudest – Error localisation could be high for this case

Figure 44: Test 16

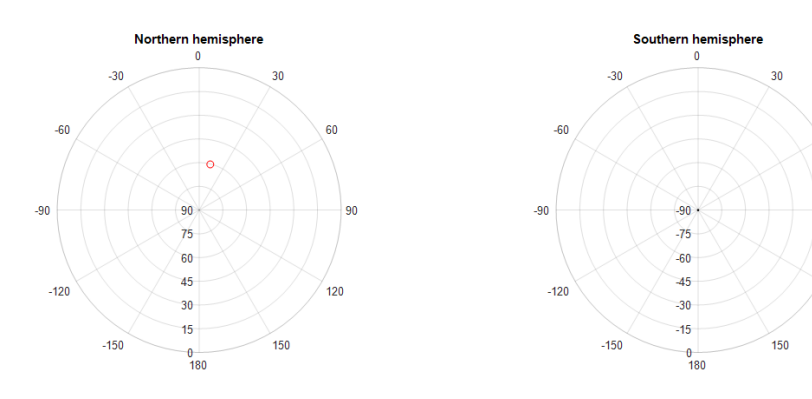




Elevation: 58.1 degrees - Azimuth: +16.7 degrees

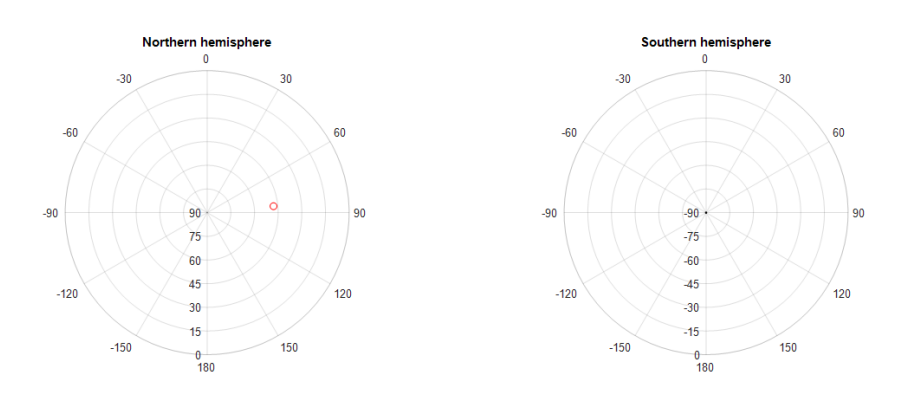
Figure 45: Test 17





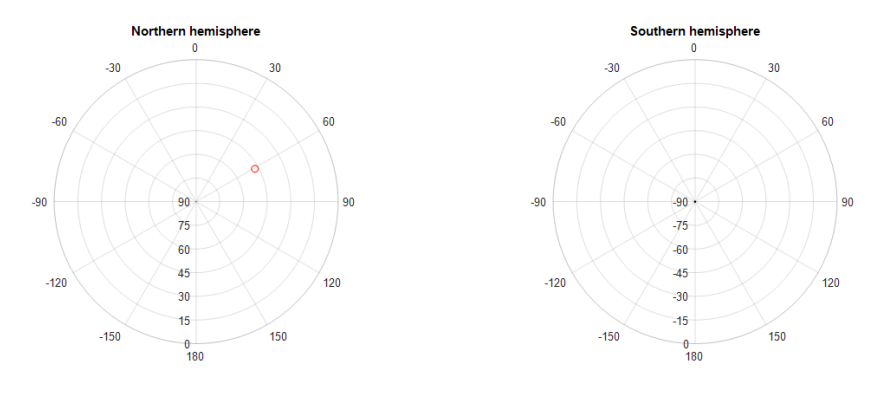
Elevation: 60.2 degrees - Azimuth: +13.7 degrees

Figure 46: Test 18



Elevation: 47.8 degrees - Azimuth: +84.4 degrees

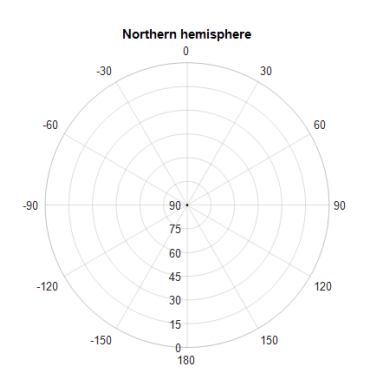
Figure 47: Test 19

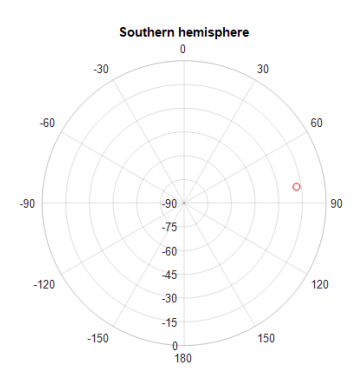


Elevation: 47.3 degrees - Azimuth: +60.8 degrees

Figure 48: Test 20

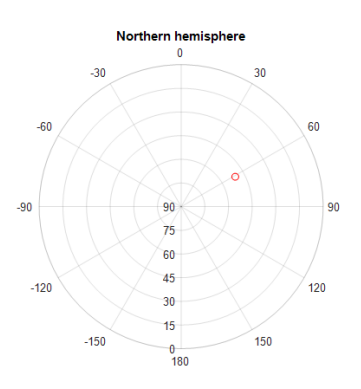


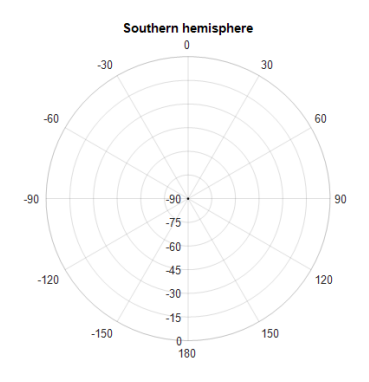




Elevation: -17.0 degrees - Azimuth: +81.8 degrees Note: Error localisation could be high in this case

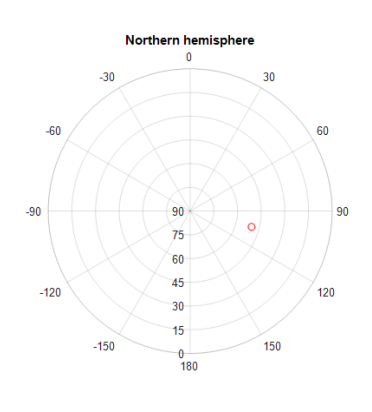
Figure 49: Test 21

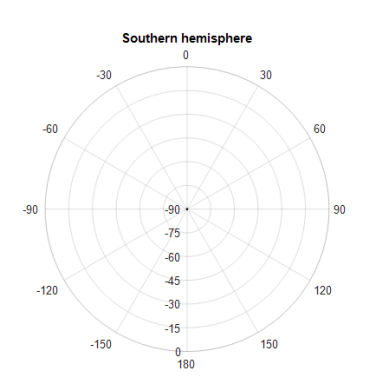




Elevation: 50.8 degrees - Azimuth: +61.1 degrees

Figure 50: Test 22

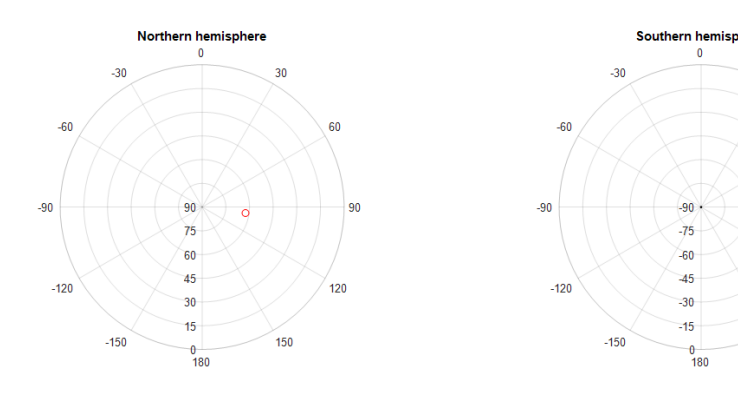




Elevation: 49.8 degrees - Azimuth: +104.4 degrees Note: Error localisation could be high in this case

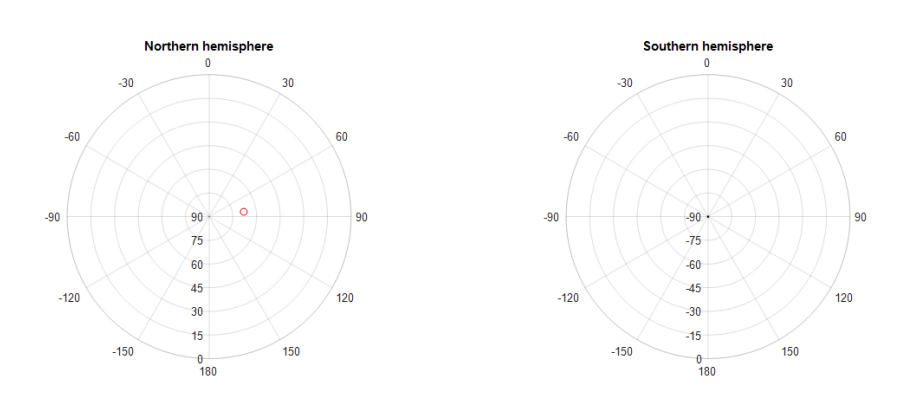
Figure 51: Test 23





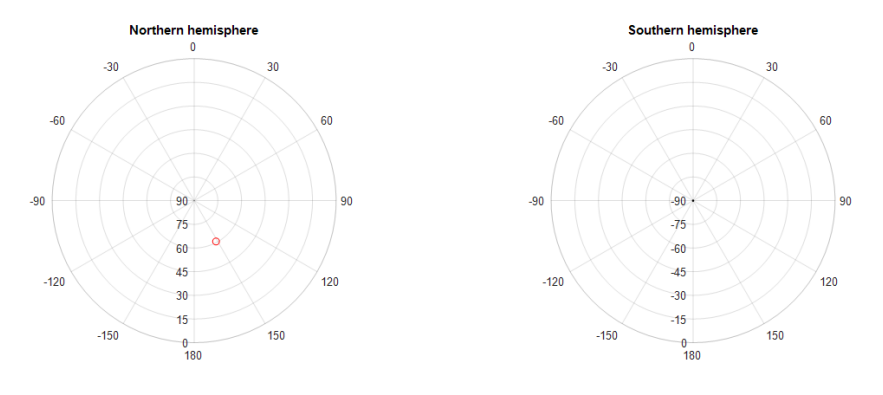
Elevation: 62.3 degrees - Azimuth: +97.8 degrees

Figure 52: Test 25



Elevation: 67.8 degrees - Azimuth: +82.0 degrees

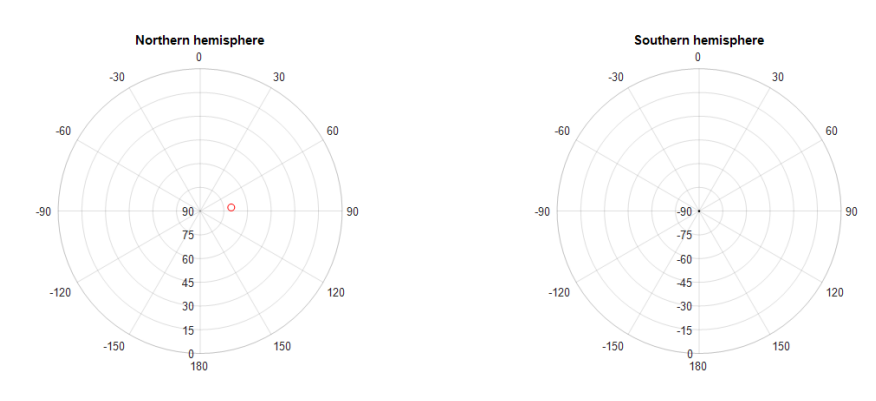
Figure 53: Test 27



Elevation: 60.7 degrees - Azimuth: +151.8 degrees

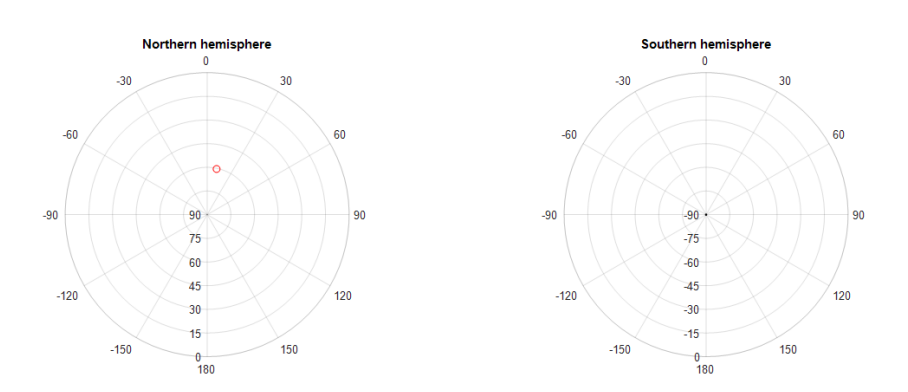
Figure 54: Test 28





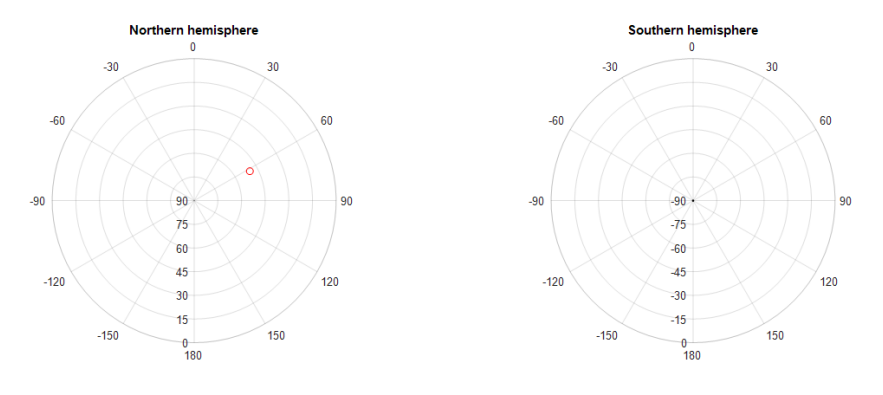
Elevation: 70.2 degrees - Azimuth: +83.2 degrees

Figure 55: Test 29



Elevation: 60.4 degrees - Azimuth: +11.6 degrees

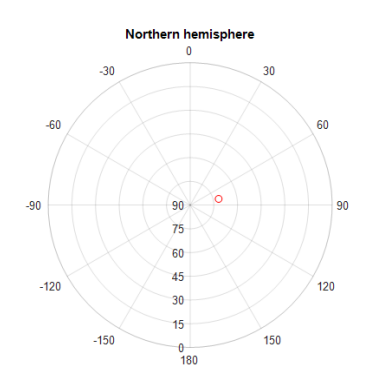
Figure 56: Test 30

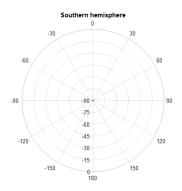


Elevation: 50.1 degrees - Azimuth: +62.1 degrees

Figure 57: Test 31

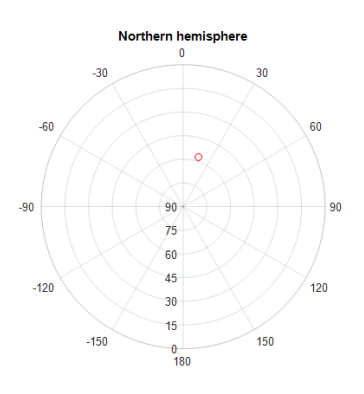


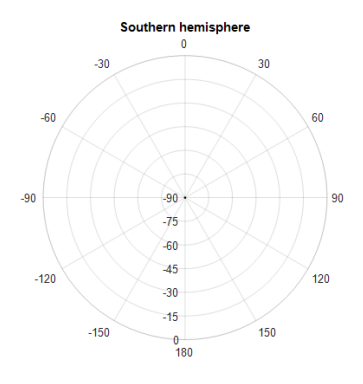




Elevation: 71.5 degrees - Azimuth: +77.7 degrees

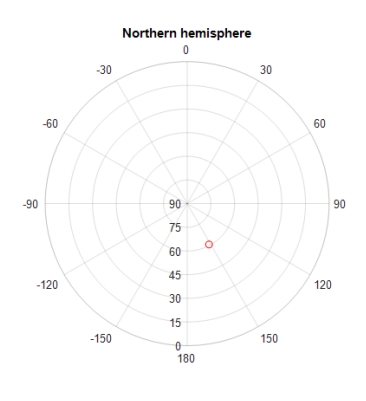
Figure 58: Test 32

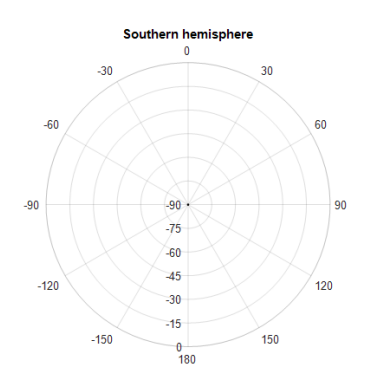




Elevation: 57.1 degrees - Azimuth: +17.2 degrees

Figure 59: Test 34

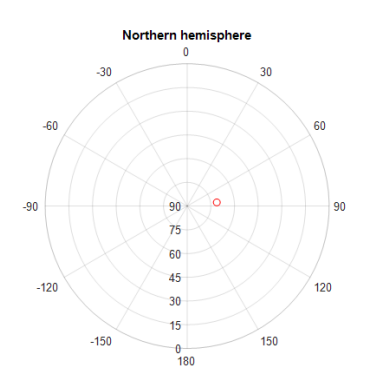


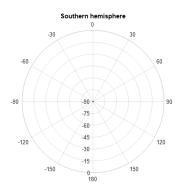


Elevation: 60.7 degrees - Azimuth: +151.8 degrees

Figure 60: Test 35

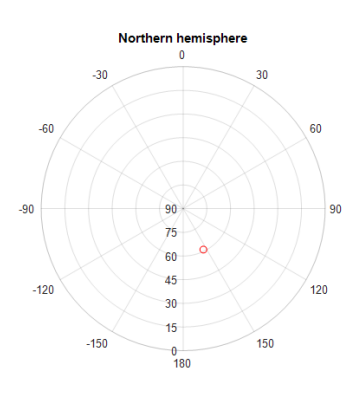


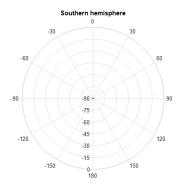




Elevation: 71.1 degrees - Azimuth: +82.9 degrees

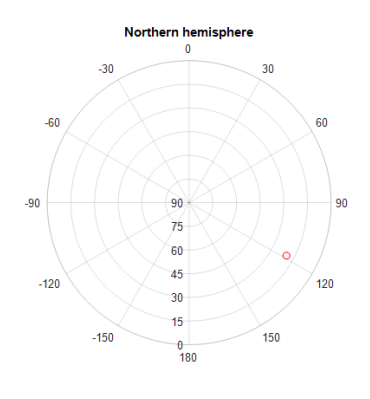
Figure 61: Test 36

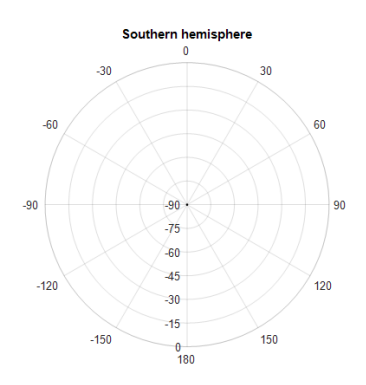




Elevation: 61.1 degrees - Azimuth: +153.7 degrees

Figure 62: Test 37

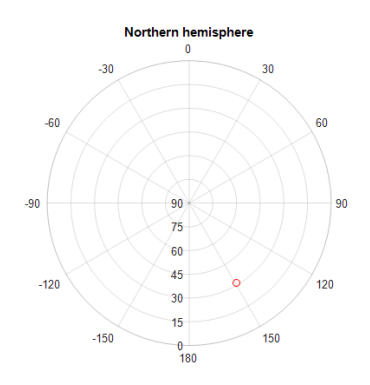


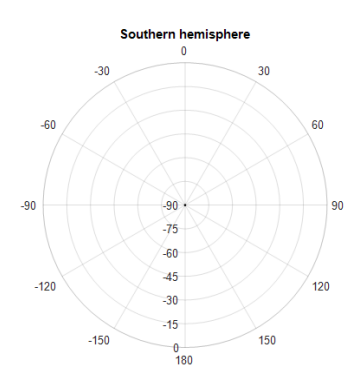


Elevation: 19.8 degrees - Azimuth: +118.6 degrees Note: This might be a reflection from another wall

Figure 63: Test 38

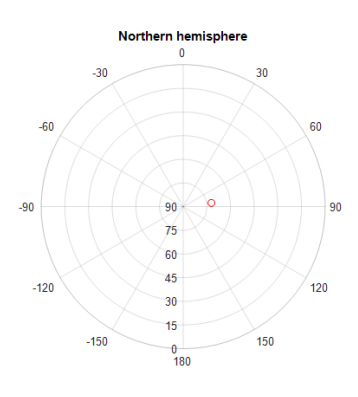


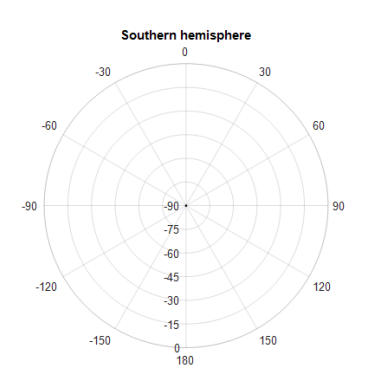




Elevation: 31.4 degrees - Azimuth: +149.3 degrees Note: Error localisation could be high in this case

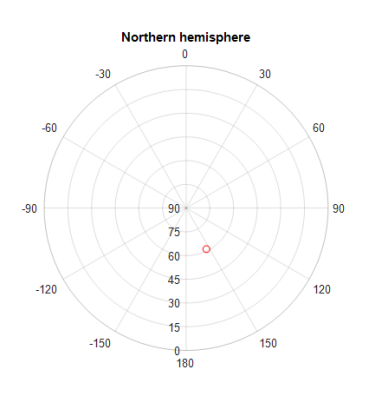
Figure 64: Test 39

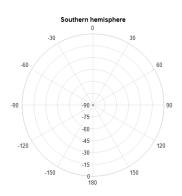




Elevation: 72.0 degrees - Azimuth: +82.5 degrees

Figure 65: Test 40

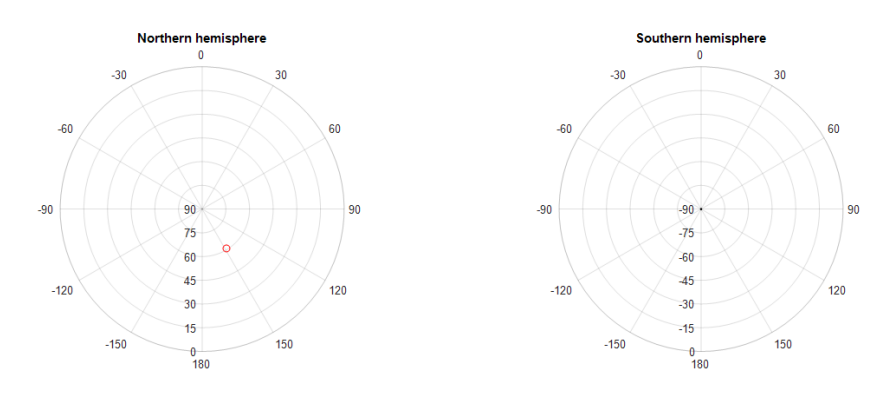




Elevation: 61.1 degrees - Azimuth: +153.7 degrees

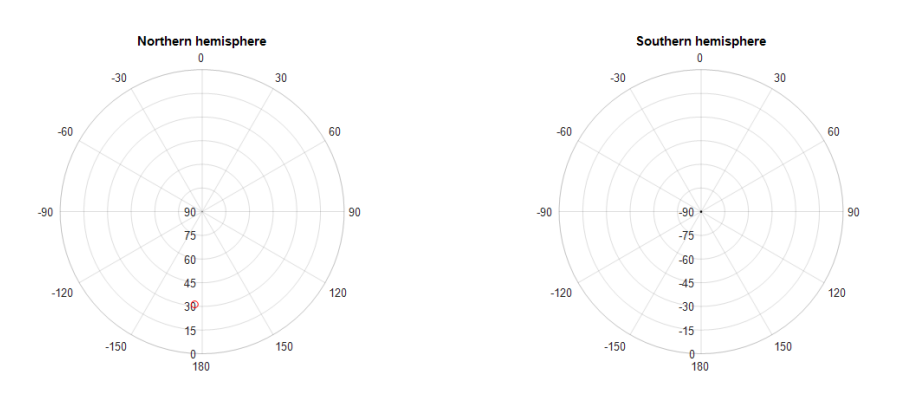
Figure 66: Test 41





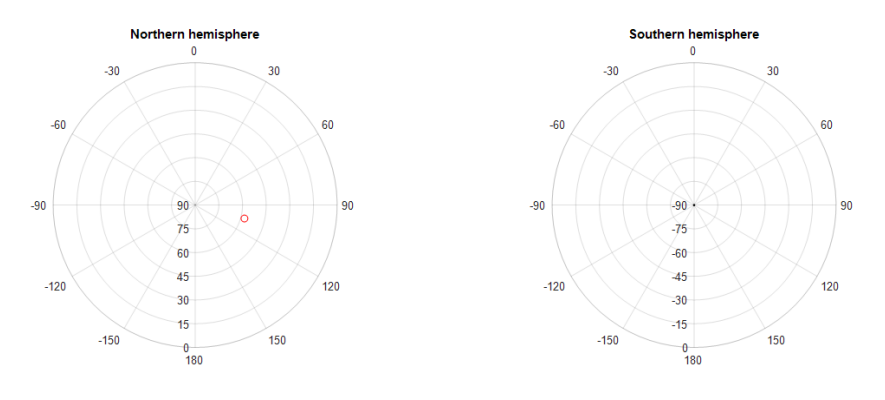
Elevation: 60.8 degrees - Azimuth: +148.3 degrees

Figure 67: Test 42



Elevation: 31.1 degrees - Azimuth: -175.4 degrees Note: Error localisation could be high in this case

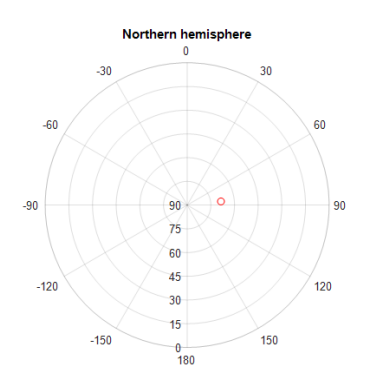
Figure 68: Test 43

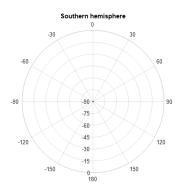


Elevation: 57.7 degrees - Azimuth: +105.2 degrees

Figure 69: Test 44 - Event 1

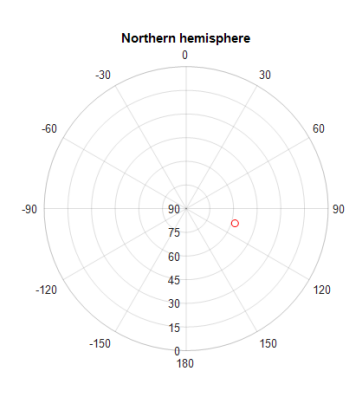


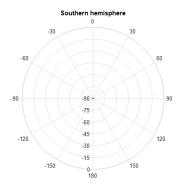




Elevation: 68.5 degrees - Azimuth: +83.8 degrees

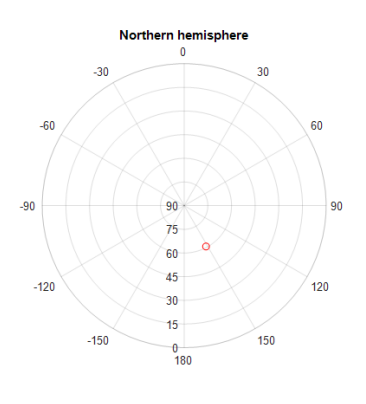
Figure 70: Test 44 - Event 2

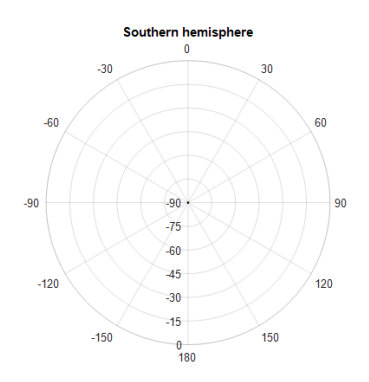




Elevation: 57.7 degrees - Azimuth: +106.7 degrees

Figure 71: Test 46

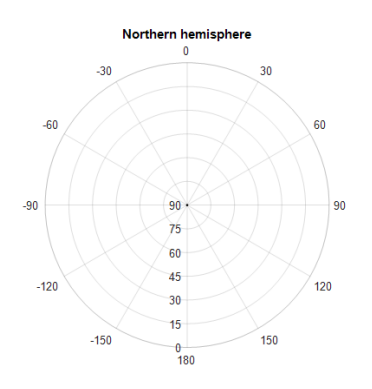


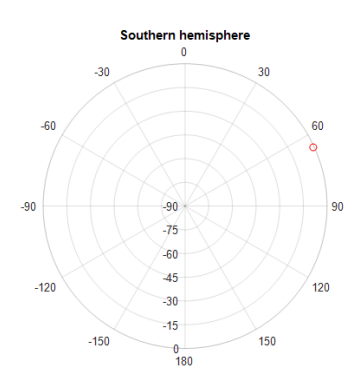


Elevation: 60.7 degrees - Azimuth: +151.8 degrees

Figure 72: Test 48

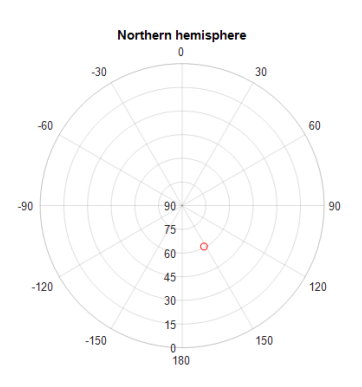


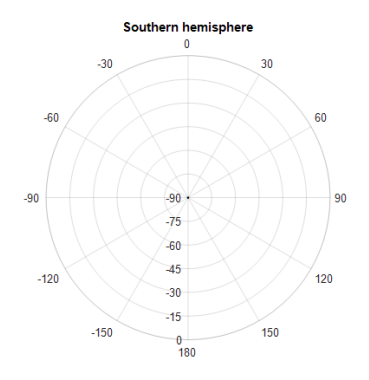




Elevation: -0.7 degrees - Azimuth: +65.4 degrees Note: Error localisation could be high in this case, this could be a reflection

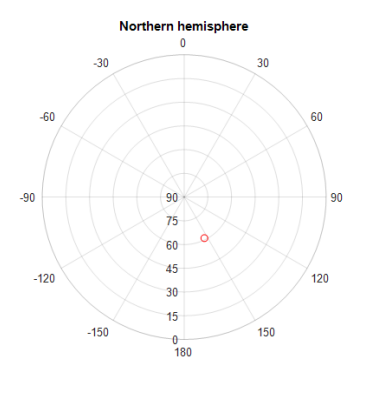
Figure 73: Test 49

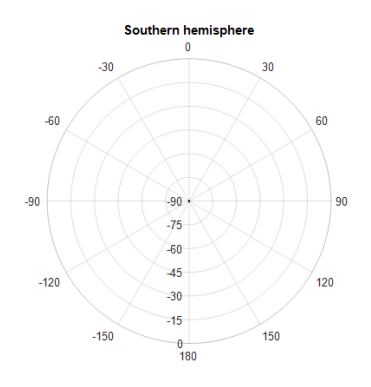




Elevation: 60.7 degrees - Azimuth: +151.8 degrees Note: Same localisation as for Test 48

Figure 74: Test 50

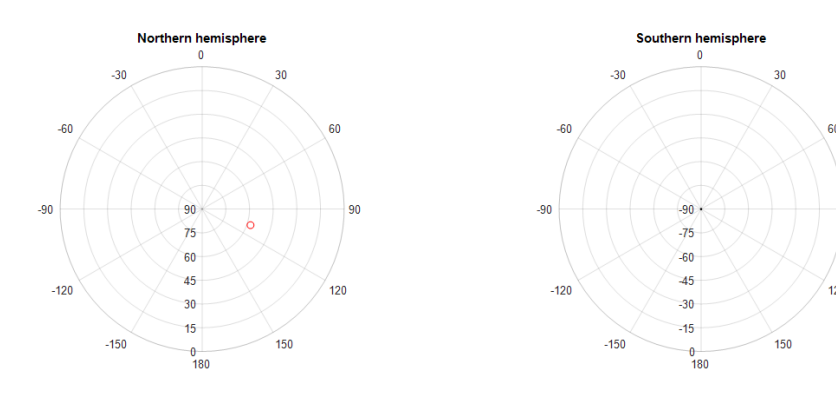




Elevation: 61.1 degrees - Azimuth: +153.7 degrees

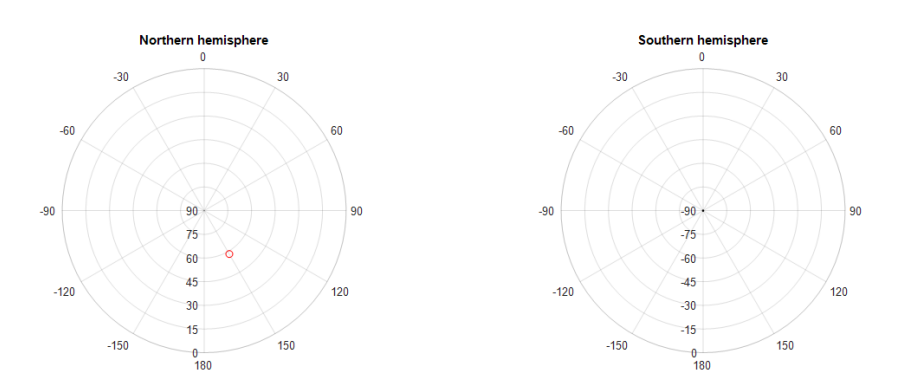
Figure 75: Test 51





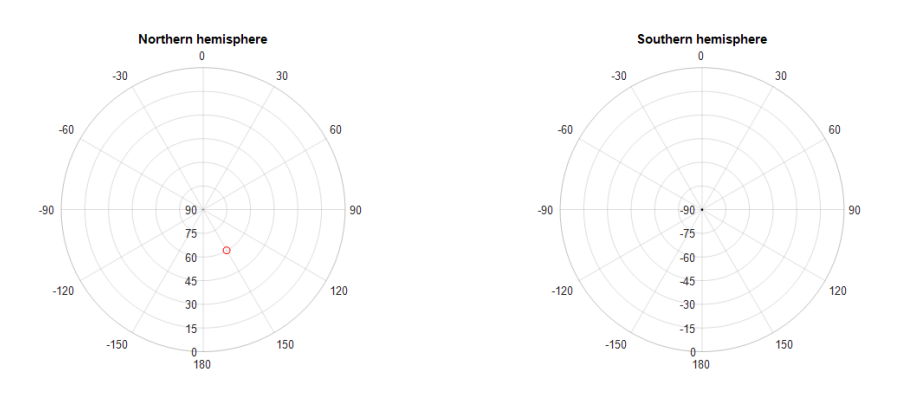
Elevation: 57.7 degrees - Azimuth: +108.3 degrees

Figure 76: Test 52



Elevation: 58.3 degrees - Azimuth: +149.9 degrees

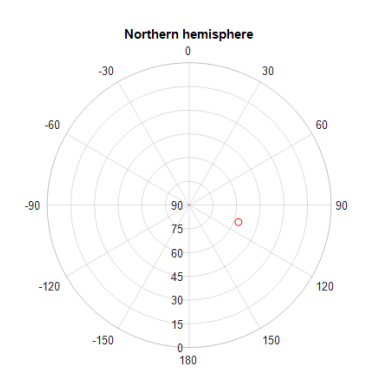
Figure 77: Test 53

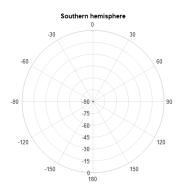


Elevation: 60.2 degrees - Azimuth: +150.0 degrees

Figure 78: Test 54

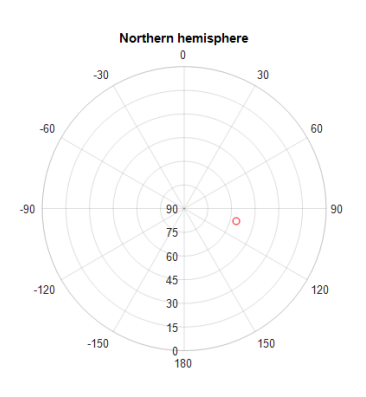


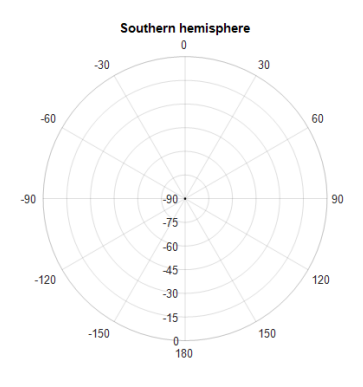




Elevation: 57.0 degrees - Azimuth: +109.0 degrees

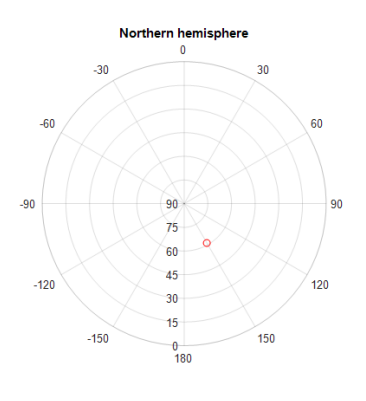
Figure 79: Test 55

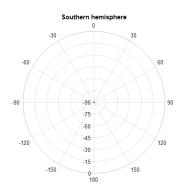




Elevation: 56.1 degrees - Azimuth: +103.5 degrees

Figure 80: Test 56

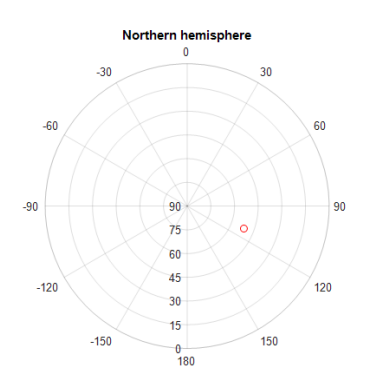


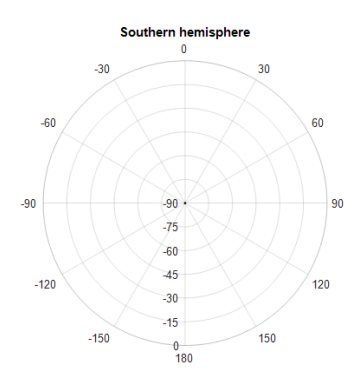


Elevation: 61.2 degrees - Azimuth: +150.1 degrees

Figure 81: Test 57

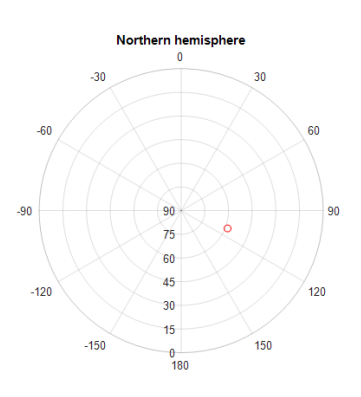


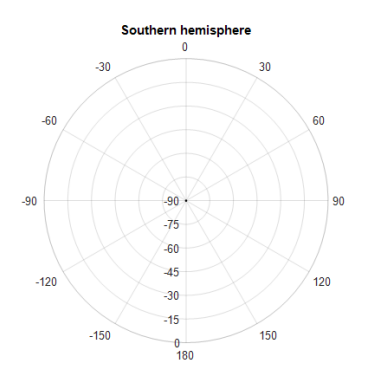




Elevation: 51.3 degrees - Azimuth: +111.5 degrees Note: Error localisation could be high in this case

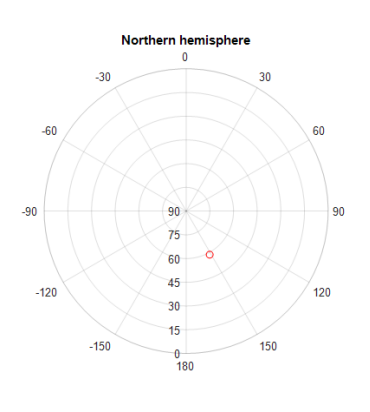
Figure 82: Test 58

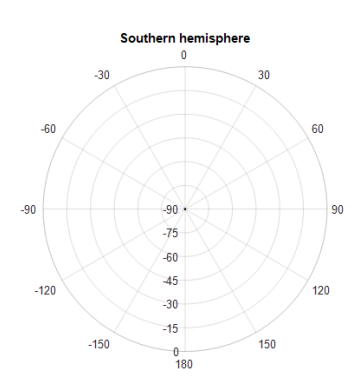




Elevation: 58.5 degrees - Azimuth: +110.9 degrees

Figure 83: Test 60

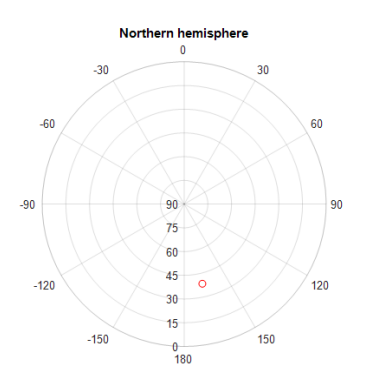


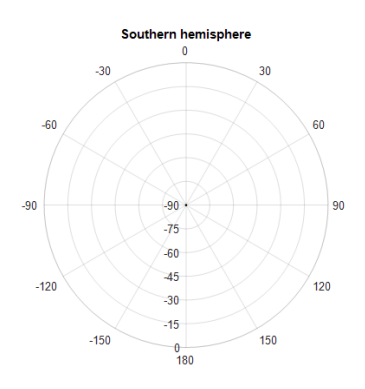


Elevation: 58.7 degrees - Azimuth: +151.6 degrees

Figure 84: Test 61

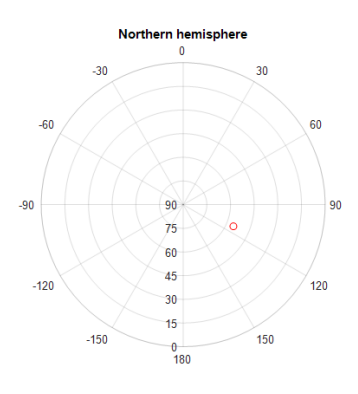


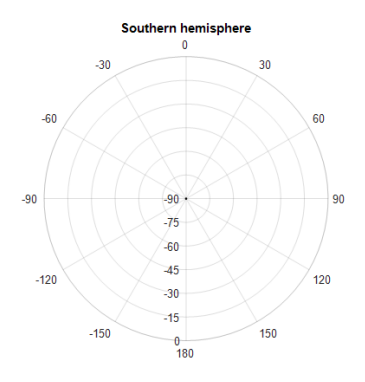




Elevation: 38.4 degrees - Azimuth: +167.1 degrees Note: Error localisation could be high in this case

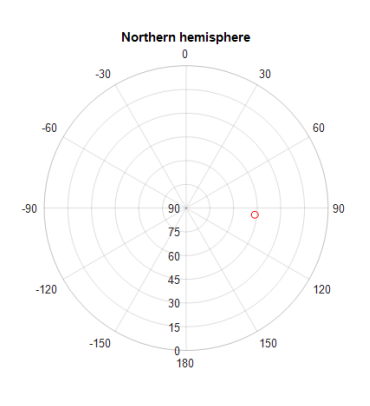
Figure 85: Test 62

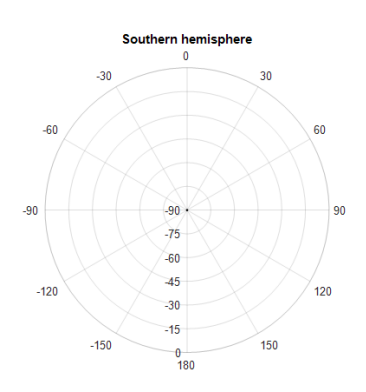




Elevation: 55.3 degrees - Azimuth: +113.3 degrees

Figure 86: Test 63

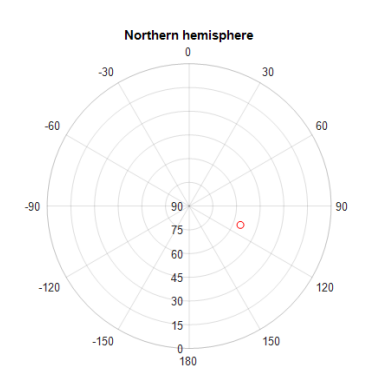


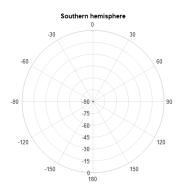


Elevation: 46.3 degrees - Azimuth: +95.5 degrees Note: Error localisation could be high in this case

Figure 87: Test 65

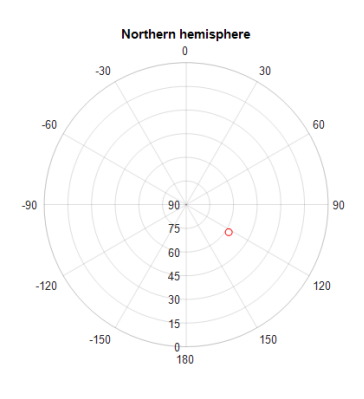


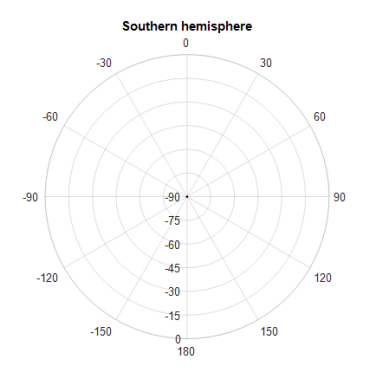




Elevation: 55.4 degrees - Azimuth: +110.2 degrees

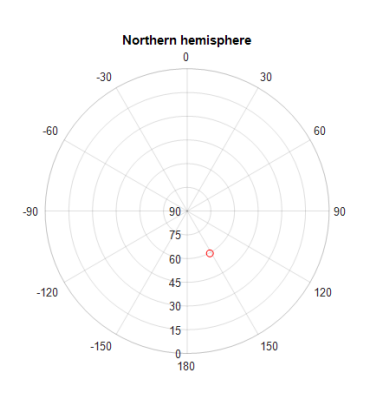
Figure 88: Test 66

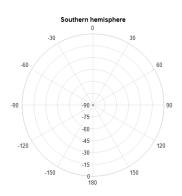




Elevation: 57.9 degrees - Azimuth: +122.8 degrees Note: Error localisation could be high in this case

Figure 89: Test 67

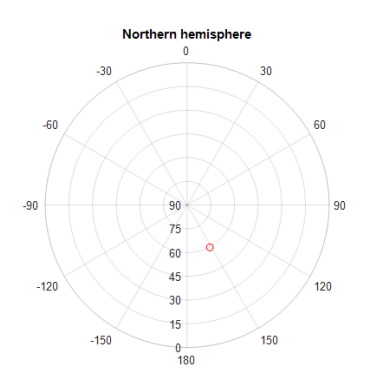


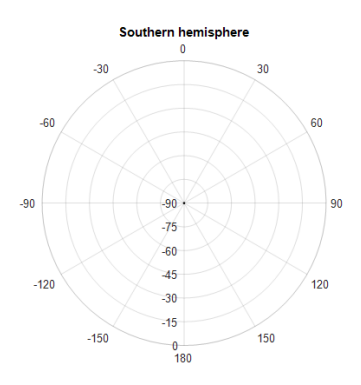


Elevation: 59.7 degrees - Azimuth: +151.7 degrees

Figure 90: Test 68

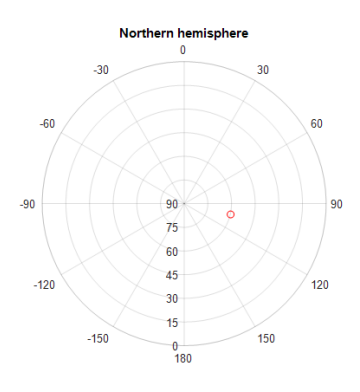


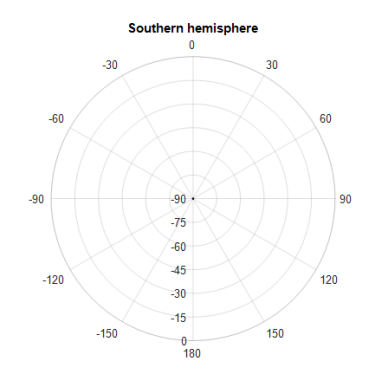




Elevation: 59.7 degrees - Azimuth: -151.7 degrees Note: Same localisation as for Test 68

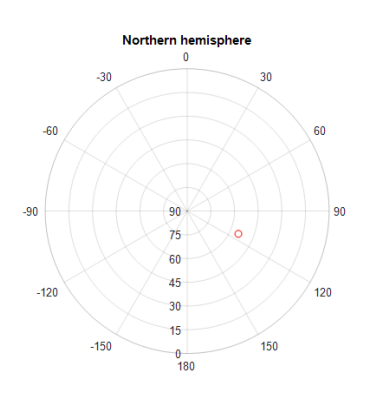
Figure 91: Test 69

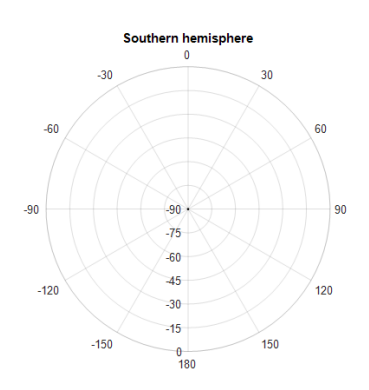




Elevation: 59.8 degrees - Azimuth: +103.0 degrees

Figure 92: Test 70

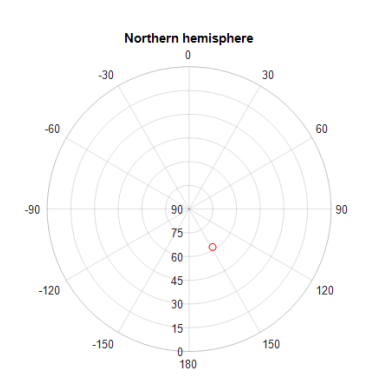


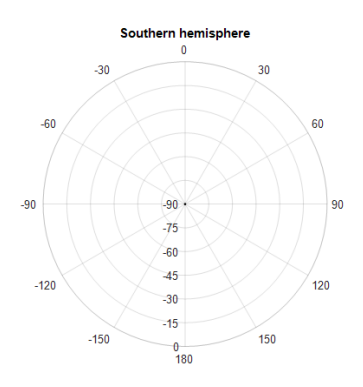


Elevation: 54.5 degrees - Azimuth: +113.9 degrees Note: Error localisation could be high in this case

Figure 93: Test 71

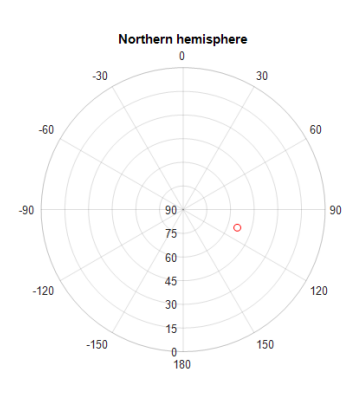


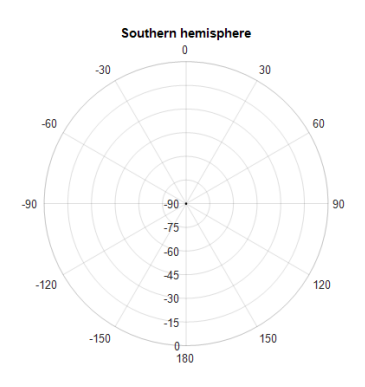




Elevation: 61.8 degrees - Azimuth: +148.3 degrees

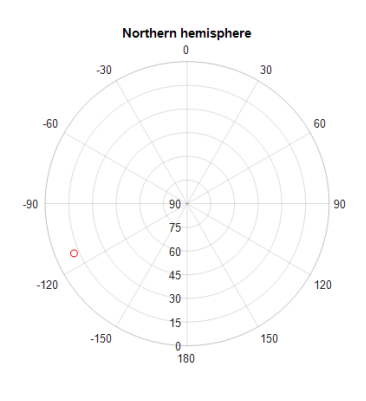
Figure 94: Test 72

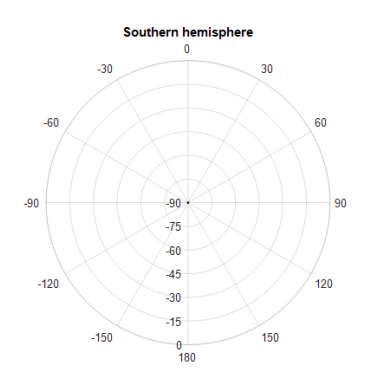




Elevation: 53.8 degrees - Azimuth: +108.4 degrees

Figure 95: Test 73

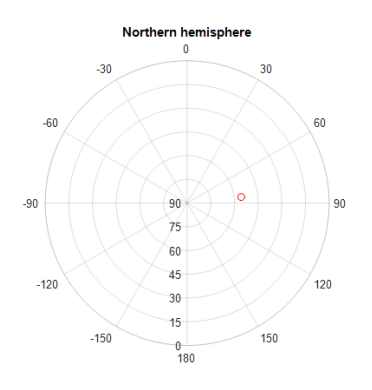


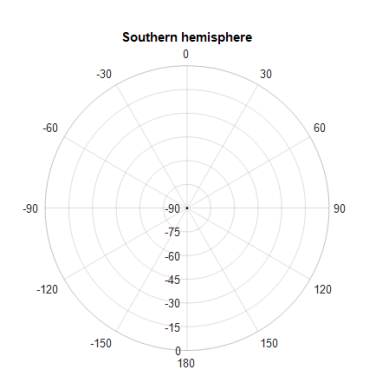


Elevation: 11.7 degrees - Azimuth: -113.7 degrees Note: Error localisation could be high in this case, this could be a reflection

Figure 96: Test 74

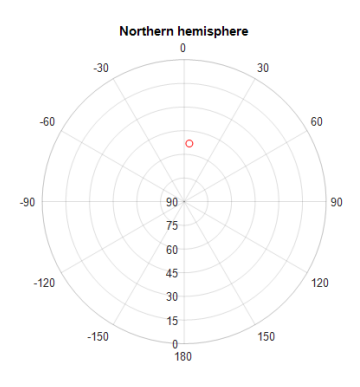


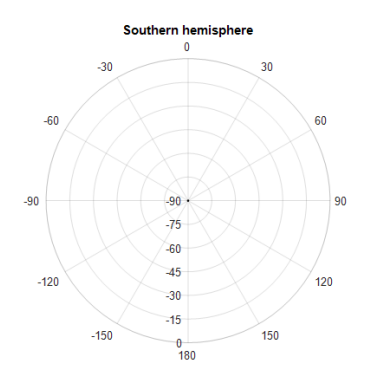




Elevation: 55.5 degrees - Azimuth: +83.6 degrees Note: Error localisation could be high in this case

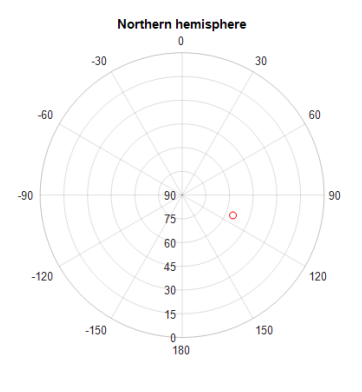
Figure 97: Test 75

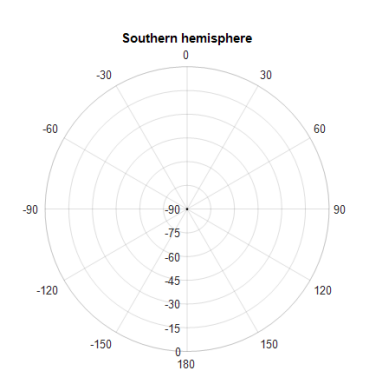




Elevation: 53.0 degrees - Azimuth: +5.0 degrees Note: Error localisation could be high in this case

Figure 98: Test 77

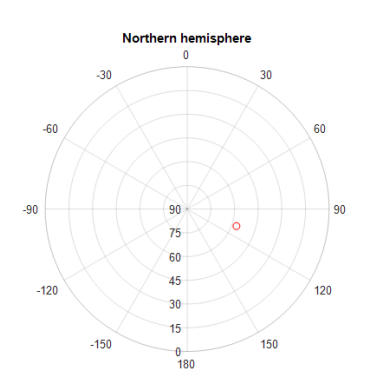


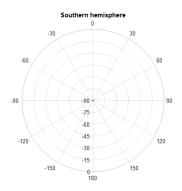


Elevation: 55.4 degrees - Azimuth: +111.7 degrees

Figure 99: Test 78

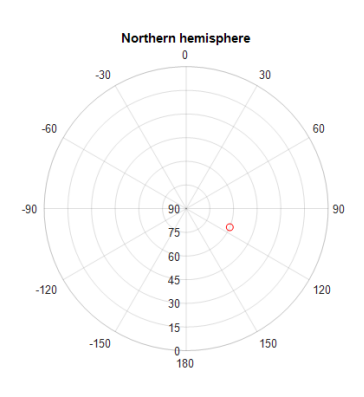


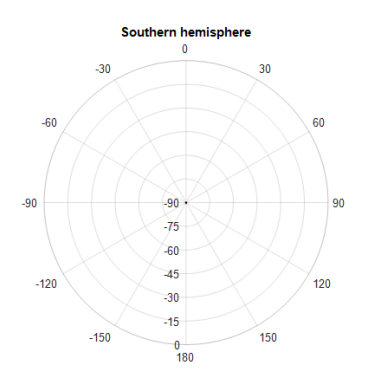




Elevation: 57.0 degrees - Azimuth: +109.0 degrees

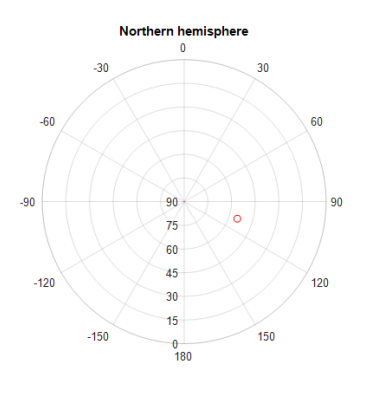
Figure 100: Test 79

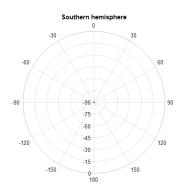




Elevation: 60.0 degrees - Azimuth: +113.1 degrees

Figure 101: Test 80

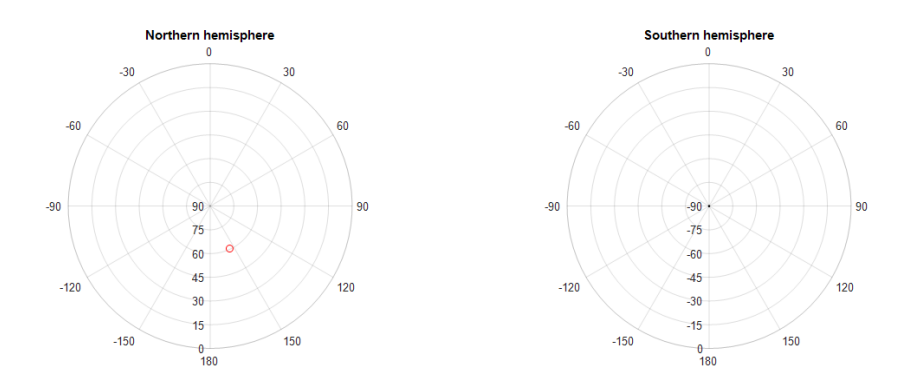




Elevation: 54.6 degrees - Azimuth: +107.8 degrees

Figure 102: Test 81





Elevation: 60.4 degrees - Azimuth: +155.4 degrees

Figure 103: Test 83



ACOUSTIC EMISSION DETECTION AND SOURCE LOCATION

When under pressure, a building emits sound events related to mechanical changes in the structure. It is important to track and localise these structural changes, for the maintenance and the safety of the building.

For this purpose, an array of microphones has been designed and developed by Doc. Peter Ulriksen from Lunds Universitet. The recorded signals have then been processed by Karim Haddad from Brüel & Kjær Sound & Vibration Measurement A/S. The processing consists in providing the localisation of a set of events.

The microphone array consists of 4 microphones arranged to locate an acoustic event in the 3D space. The processing is based on cross-correlations between pairs of microphones.

In total, 75 events have been analysed. A very large majority of localised events concern the top hemisphere above the position of the microphone array. A few numbers of events seem to be coming from the lower part, below the microphone array, but for these cases the results are less accurate.

Energiforsk is the Swedish Energy Research Centre – an industrially owned body dedicated to meeting the common energy challenges faced by industries, authorities and society. Our vision is to be hub of Swedish energy research and our mission is to make the world of energy smarter!

